JM PAPERS

Enhancement of wave transmissions in multiple radiative and convective zones

Tao Cai[1,†], **Cong Yu**[1,2,†] **and Xing Wei**[3]

[1]State Key Laboratory of Lunar and Planetary Sciences, Macau University of Science and Technology, Macau, PR China

[2]School of Physics and Astronomy, Sun Yat-sen University, Zhuhai 519082, PR China

[3]Department of Astronomy, Beijing Normal University, Beijing 100875, PR China

In this paper, we study wave transmission in a rotating fluid with multiple alternating convectively stable and unstable layers. We have discussed wave transmissions in two different circumstances: cases where the wave is propagative in each layer and cases where wave tunnelling occurs. We find that efficient wave transmission can be achieved by 'resonant propagation' or 'resonant tunnelling', even when stable layers are strongly stratified, and we call this phenomenon 'enhanced wave transmission'. Enhanced wave transmission only occurs when the total number of layers is odd (embedding stable layers are alternatingly embedded within clamping convective layers, or *vice versa*). For wave propagation, the occurrence of enhanced wave transmission requires that the clamping layers have similar properties, the thickness of each clamping layer is close to a multiple of the half-wavelength of the corresponding propagative wave and the total thickness of the embedded layers is close to a multiple of the half-wavelength of the corresponding propagating wave (resonant propagation). For wave tunnelling, we have considered two cases: tunnelling of gravity waves and tunnelling of inertial waves. In both cases, efficient tunnelling requires that the clamping layers have similar properties, the thickness of each embedded layer is much smaller than the corresponding e-folding decay distance and the thickness of each clamping layer is close to a multiple-and-a-half of the half-wavelength (resonant tunnelling).

Key words: rotating flows, stratified flows, waves in rotating fluids

1. Introduction

Inertial and gravito-inertial waves are important phenomena in rotating stars and planets. Wave propagation can transport momentum and energy, therefore it may have significant

† Email addresses for correspondence: tcai@must.edu.mo, yucong@mail.sysu.edu.cn

impact on stellar or planetary structures and evolutions. For example, internal-gravity waves (IGWs) play an important role in transporting angular momentum when they propagate in the radiative zones of stars (Belkacem *et al.* 2015*a*, ; Pinçon *et al.* 2017; Aerts, Mathis & Rogers 2019). Study reveals that IGWs can reduce differential rotation in low mass stars in a short time scale (Rogers *et al.* 2013). They can also explain the misalignment of exoplanets around hot stars (Rogers, Lin & Lau 2012). Apart from IGWs, inertial waves can also be generated in rotating planets (Ogilvie & Lin 2004; Wu 2005*a*; Goodman & Lackner 2009). It has been found that the resonantly excited inertial wave has an important impact on the tidal dissipation in planets (Wu 2005*b*).

It is quite common for a star or planet to have a multi-layer structure. For example, a superadiabatic region embedded in radiative layers may appear in a neutron star's atmosphere because of the ionization of ^{56}Fe (Miralles, Urpin & Van Riper 1997). Waves generated by convective motions can transport energy to the chromosphere and corona, which may drive the stellar wind. In A-type stars, it is possible for them to have complex internal structures with multiple convection zones. Interaction between these convective zones has important implications in material mixing and energy transport (Silvers & Proctor 2007). It is also known that layered semiconvection zones can be formed in stars in the process of double-diffusive convection (Mirouh *et al.* 2012; Wood, Garaud & Stellmach 2013; Garaud 2018). For main sequence stars slightly more massive than the Sun, it has been found that the efficiency of mixing in layered semiconvection zones sensitively depends on the layer height (Moore & Garaud 2016). Layered convection zones also exist in planets. Multi-layer structure has been detected in a region several hundred metres below the surface of the Arctic ocean (Rainville & Winsor 2008). Observation shows that a shallow convective region is embedded within stable layers in the atmosphere of Venus (Tellmann *et al.* 2009). Seismology on Saturn's ring reveals the layered stable stratification in the deep interior of Saturn (Fuller 2014). If stable stratification exists in the deep interior of Saturn, then the g-mode can be excited in this region. Layered convection probably also exists in Jupiter. A new model with layered convection on Jupiter and Saturn indicates that the heavy elements in our Jovian planets are more enriched than previously thought (Leconte & Chabrier 2012). One interesting question is whether g-mode waves can transmit to the surface, so that they can be possibly captured by observations.

Wave can transmit in a double barrier system through a tunnelling process. Sutherland & Yewchuk (2004) studied transmissions of internal wave tunnelling for both N^2-barrier (low N^2 layer embedded in high N^2 layers and horizontal mean density varies continuously) and mixed-N^2 (low N^2 layer embedded in high N^2 layers but horizontal mean density varies discontinuously) profiles, where N^2 is the square of the buoyancy frequency. They found that wave transmission can be efficient for resonant transfers. Sutherland (2016) investigated the transmission of internal waves in a multi-layer structure separated by discontinuous density jumps. He deduced an analytical solution for wave transmission when the steps are evenly spaced, and predicted that waves with longer horizontal wavelength and larger frequencies are more likely to transmit in the density staircase profile. Sutherland (1996) considered wave propagation in profiles of piecewise linear stratified layers with weaker stratification at the top. He discovered that large-amplitude IGWs incident from the bottom can partially transmit energy into the top layer by the generation of a lower frequency wave packet. Resonant tunnelling of electron transmission in double barriers is familiar in quantum physics, and has been widely used in designing semiconductor devices, such as tunnel diodes, NPN (negative–positive–negative) and PNP (positive–negative–positive) triodes (Singh 2010). In comparison with tunnelling

of electron transmission, it is expected that resonant tunnelling also occurs for wave transmission in multi-layer structures.

Wave transmission in a three-layer structure with rotational effects has been considered by Gerkema & Exarchou (2008). They compared wave transmissions with and without traditional approximations (the horizontal component of rotation is neglected when the traditional approximation is adopted on an f-plane). For a three-layer structure with a convective layer embedded in strongly stratified layers, waves cannot survive in both convective and stratified layers under the traditional approximation, while it is possible if non-traditional effects are taken into account. They also showed that near-inertial waves are always transmitted efficiently for stratified layers of any stratification. Belyaev, Quataert & Fuller (2015) investigated the free modes of a multi-layer structure wave propagation with rotation at the poles and equator. They found that g-modes with vertical wavelengths smaller than the layer thickness are evanescent. André, Barker & Mathis (2017) studied the effects of rotation on free modes and wave transmission in a multi-layer structure at a general latitude. They showed that transmission can be efficient when the incident wave is resonant with waves in adjacent layers with half-wavelengths equal to the layer depth. They also discovered that perfect wave transmission can be obtained at the critical latitude. Pontin *et al.* (2020) studied the wave propagation in semiconvective regions of non-rotating giant planets in the full sphere. They found that wave transmissions are efficient for very large wavelength waves.

In previous works (Wei 2020*a*,*b*; Cai, Yu & Wei 2021), we have discussed the efficiency of inertial and gravito-inertial wave transmissions in a two-layer structure on f-planes. For a step stratification near the interface, we have found that the transmission generally is not efficient if the stable layer is strongly stratified. In this paper, we investigate the wave transmission in a multi-layer structure on f-planes. Specifically, we will consider wave transmissions via two different mechanisms: wave propagation and wave tunnelling. We find that wave transmission in a multi-layer structure can be significantly different from that in a two-layer structure.

2. The model and result

For the Boussinesq flow in a rotating f-plane, the hydrodynamic equations can be synthesized into a partial differential equation on vertical velocity w (Gerkema & Shrira 2005*b*)

$$\nabla^2 w_{tt} + (\mathbf{f} \cdot \nabla)^2 w + N^2(z)\nabla_h^2 w = 0, \tag{2.1}$$

where $\mathbf{f} = (0, \tilde{f}, f)$ is the vector of Coriolis parameters, N^2 is the square of the buoyancy frequency, ∇^2 is Laplacian operator, ∇_h^2 is its horizontal component and the subscript t represents taking the derivative with respect to time. By letting $w = W(\chi, z) \exp(-i\sigma t)$, Gerkema & Shrira (2005*b*) found (2.1) can be transformed into the following equation:

$$AW_{\chi\chi} + 2BW_{\chi z} + CW_{zz} = 0, \tag{2.2}$$

where $A = \tilde{f}_s^2 - \sigma^2 + N^2$, where σ is the time frequency, $B = f\tilde{f}_s$, $C = f^2 - \sigma^2$, $\tilde{f}_s = \tilde{f} \sin\alpha$, where α is the angle between the direction of the plane wave and the x-direction, and χ is a variable satisfying $x = \chi \cos\alpha$ and $y = \chi \sin\alpha$. Here, x, y, z are the west–east, south–north and vertical directions, respectively. We define $A_0 = \tilde{f}_s^2 - \sigma^2$, so that $A = A_0 + N^2$. Taking advantage of plane waves and assuming $W(\chi, z) = \psi(z) \exp(i\delta z + ik\chi)$, Gerkema & Shrira (2005*b*) have further simplified (2.2) into an equation of

wave amplitude ψ

$$\psi_{zz} + k^2 \frac{B^2 - AC}{C^2} \psi = 0, \tag{2.3}$$

where $\delta = -kB/C$, with k is the horizontal wavenumber. A wave solution then requires $B^2 - AC > 0$, and the squared wavenumber is $r^2 = k^2(B^2 - AC)/C^2$. If $B^2 - AC > 0$, then r is a real number and the flow propagates along the vertical direction as a wave. On the other hand, if $B^2 - AC < 0$, then r is a pure imaginary number, and the wave amplitude increases or decreases exponentially.

In previous works (Wei 2020*a*; Cai *et al.* 2021) we have investigated wave transmission in a two-layer setting f-plane (a convective layer with $N^2 = 0$ and a convectively stable layer with $N^2 > 0$). Note that the actual N^2 should be smaller than zero. In real stars, however, convection is generally efficient in transporting energy, leading to a nearly adiabatic thermal structure. Thus, N^2 values in convective layers are only slightly smaller than zero. For this reason, we choose $N^2 = 0$ for convective layers in our model. In this paper, we extend previous works to study the wave transmission in a multi-layer setting f-plane. At this beginning stage, we use an ideal model by assuming N^2 is constant in each layer. In all convective layers, N^2 values are equal and set to zero. In stable layers, N^2 values can be different but remain constant in each layer, with minimum and maximum values of N_{min}^2 and N_{max}^2, respectively. We also assume that the propagation of inertial waves is not affected by convection. The validity of this assumption requires that the nonlinear and viscous effects are small. Detailed discussion on relations and differences between convection and inertial waves can be found in Zhang & Liao (2017). Here, we attempt to use a toy model to gain some insights into wave transmissions in a multi-layer structure. Cai *et al.* (2021) have made a detailed discussion on the frequency domain of wave solutions. If a wave is to survive in a convective layer, then the following condition must be satisfied:

$$\Delta_c = B^2 - A_0 C > 0. \tag{2.4}$$

Similarly, the condition for wave propagation in a stable layer is

$$\Delta_s = B^2 - A_0 C - N_s^2 C > 0. \tag{2.5}$$

Let us define

$$\sigma_{1,4}^2 = \left[(f^2 + \tilde{f}_s^2) \mp \sqrt{(f^2 + \tilde{f}_s^2)^2} \right] \Big/ 2, \tag{2.6}$$

$$\sigma_{2,5}^2 = \left[(f^2 + \tilde{f}_s^2 + N_{min}^2) \mp \sqrt{(f^2 + \tilde{f}_s^2 + N_{min}^2)^2 - 4N_{min}^2 f^2} \right] \Big/ 2, \tag{2.7}$$

$$\sigma_{3,6}^2 = \left[(f^2 + \tilde{f}_s^2 + N_{max}^2) \mp \sqrt{(f^2 + \tilde{f}_s^2 + N_{max}^2)^2 - 4N_{max}^2 f^2} \right] \Big/ 2, \tag{2.8}$$

where $\sigma_1 = 0$ and $\sigma_4 = f^2 + \tilde{f}_s^2$ are roots of $\Delta_c = 0$, and $\sigma_{2,5}$ and $\sigma_{3,6}$ are roots of $\Delta_s = 0$ when $N_s^2 = N_{min}^2$ and $N_s^2 = N_{max}^2$, respectively. It is not difficult to verify that the relation $\sigma_1 \leq \sigma_2 \leq \sigma_3 \leq \sigma_4 \leq \sigma_5 \leq \sigma_6$ holds.

Figure 1(*a*) shows the frequency ranges for different waves in convectively unstable and stable layers, respectively. In the green region ($\sigma_3^2 < \sigma^2 < \sigma_4^2$), waves can survive and propagate in both convective and stable layers, and we term this phenomenon
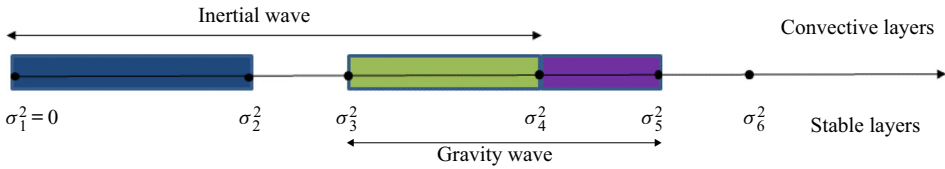
Figure 1. Plot of wave propagations in multiple convectively stable and unstable layers. Wave frequency ranges are shown above and below the middle arrow for convective and stable layers, respectively. Wave propagation occurs in the green region, tunnelling of inertial wave occurs in the blue region and tunnelling of gravity wave occurs in the purple region.
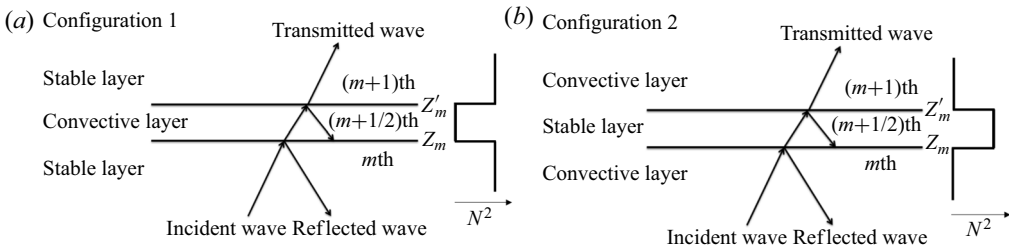

Figure 2. Plots of wave propagations in multiple convectively stable and unstable layers. (*a*) The convective layer is embedded between two stable layers. (*b*) The stable layer is embedded between two convective layers. Structure of the square of buoyancy frequency N^2 is shown by the side.

'wave propagation'. In the blue region $\sigma_1^2 < \sigma^2 < \sigma_2^2$, inertial waves can survive in convective layers but gravity waves cannot survive in stable layers. Inertial waves can transmit through a tunnelling process, and we term this phenomenon 'tunnelling of inertial wave'. In the purple region $\sigma_4^2 < \sigma^2 < \sigma_5^2$, gravity waves can survive in stable layers but inertial waves cannot survive in convective layers. Similarly, gravity waves can transmit through a tunnelling process, and we term this phenomenon 'tunnelling of gravity wave'.

In Cai *et al.* (2021), we have also deduced that $c_{p0}c_g$ has the same sign as C, where c_{p0} is the modified vertical component of wave phase velocity and c_g is the vertical component of the wave group velocity. The vertical component of phase velocity should be computed by $\sigma/(\delta \pm r)$, but here the tilted effect is excluded in the modified one $c_{p0} = \sigma/(\pm r)$. Since the wave direction of energy propagation is determined by c_g, a proper choice of wave direction depends on whether the wave is sub-inertial ($C > 0$) or super-inertial ($C < 0$).

2.1. *Wave propagation*

In this section, we discuss wave propagation in both convective and stable layers, which requires that the frequency is in the range $\sigma_3^2 < \sigma^2 < \sigma_4^2$. We consider different configurations with different combinations of layer structures and wave directions. The incident wave can propagate from the convective layer or stable layer, and the wave propagating direction can be upward or downward. Since up/down symmetry holds in Boussinesq flow, it is sufficient to discuss the cases with waves incident from the bottom. The cases with waves incident from the top can be inferred from the up/down symmetry. Figure 2 shows plots of the two configurations in a three-layer setting f-plane. Structures with more layers are similar. At each interface, two boundary conditions have to be satisfied: the vertical velocity is continuous; and the first derivative of the vertical velocity is continuous (Wei 2020*a*; Cai *et al.* 2021).

We start the discussion on configuration 1 (figure 2*a*), and assume that the number of interfaces is even. We label the convective layer with the half-grid number $(m + 1/2)$.

For the $(m + 1/2)$th convective layer, we label its lower and upper neighbouring stable layers the mth and $(m + 1)$th stable layers, respectively; and we set the locations of the lower and upper interfaces at z_m and z'_m, respectively. The thickness of the convective layer is $\Delta z'_m = z'_m - z_m$, and the thickness of the stable layer is $\Delta z_m = z_m - z'_{m-1}$. For the mth stable layer, we define its wavenumber square as $s_m^2 = k^2(B^2 - A_0 C - N_m^2 C)/C^2$. For the $(m + 1/2)$th convective layer, we define its wavenumber square as $q_m^2 = k^2(B^2 - A_0 C)/C^2$. In this paper, we only consider a simple case, in which the square of the buoyancy frequency is a constant within each convective or stable layer. Under this assumption, we find wave solutions in the mth stable layer

$$\psi_m(z) = a_m \, e^{-is_m z} + b_m \, e^{is_m z}, \quad z \in (z'_{m-1}, z_m), \tag{2.9}$$

and in the $(m + 1/2)$th convective layer

$$\psi_{m+1/2}(z) = c_m \, e^{-iq_m z} + d_m \, e^{-iq_m z}, \quad z \in (z_m, z'_m), \tag{2.10}$$

respectively. As mentioned earlier, $c_{p0} c_g$ has the same sign as C, from which we conclude $Sgn(c_g) = Sgn(C)Sgn(c_{p0})$. The sign of the modified vertical phase velocity c_{p0} is determined by the sign of q_m or s_m. If $Sgn(C)Sgn(c_{p0}) > 0$, then the vertical group velocity c_g is positive (wave direction is outgoing); on the other hand, if $Sgn(C)Sgn(c_{p0}) < 0$, then c_g is negative (wave direction is incoming). We choose $q_m > 0$ for $C > 0$, and $q_m < 0$ for $C < 0$. For either case, the waves with wavenumbers q_m and s_m are outgoing waves, and the waves with wavenumbers $-q_m$ and $-s_m$ are incoming waves. Note that all q_m and s_m always have the same sign. Matching the boundary conditions at the interfaces z_m and z'_m, we have

$$a_m \, e^{-is_m z_m} + b_m \, e^{is_m z_m} = c_m \, e^{-iq_m z_m} + d_m \, e^{iq_m z_m}, \tag{2.11}$$

$$(-a_m \, e^{-is_m z_m} + b_m \, e^{is_m z_m})s_m = (-c_m \, e^{-iq_m z_m} + d_m \, e^{iq_m z_m})q_m, \tag{2.12}$$

$$c_m \, e^{-iq_m z'_m} + d_m \, e^{iq_m z'_m} = a_{m+1} \, e^{-is_{m+1} z'_m} + b_{m+1} \, e^{is_{m+1} z'_m}, \tag{2.13}$$

$$(-c_m \, e^{-iq_m z'_m} + d_m \, e^{iq_m z'_m})q_m = (-a_{m+1} \, e^{-is_{m+1} z'_m} + b_{m+1} \, e^{is_{m+1} z'_m})s_{m+1}. \tag{2.14}$$

Wave propagations in multi-layer structures have been investigated in Belyaev *et al.* (2015), André *et al.* (2017) and Pontin *et al.* (2020). A useful approach to modelling wave propagations in a multi-layer structure is to build on relations of wave amplitudes by transfer matrices. From the above boundary conditions, we can derive the following transfer relations (see Appendix A):

$$\begin{bmatrix} a_m \\ b_m \end{bmatrix} = \boldsymbol{T}_{m,m+1} \begin{bmatrix} a_{m+1} \\ b_{m+1} \end{bmatrix} = \begin{bmatrix} \hat{T}_{11} & \hat{T}_{12} \\ \hat{T}_{21} & \hat{T}_{22} \end{bmatrix} \begin{bmatrix} a_{m+1} \\ b_{m+1} \end{bmatrix}, \tag{2.15}$$

where

$$\hat{T}_{11} = \frac{1}{4} \, e^{i(s_m z_m - s_{m+1} z'_m)} \left[\left(1 + \frac{q_m}{s_m} + \frac{s_{m+1}}{s_m} + \frac{s_{m+1}}{q_m} \right) e^{iq_m \Delta z'_m} \right.$$
$$\left. + \left(1 - \frac{q_m}{s_m} + \frac{s_{m+1}}{s_m} - \frac{s_{m+1}}{q_m} \right) e^{-iq_m \Delta z'_m} \right], \tag{2.16}$$

$$\hat{T}_{12} = \frac{1}{4} \, e^{i(s_m z_m + s_{m+1} z'_m)} \left[\left(1 + \frac{q_m}{s_m} - \frac{s_{m+1}}{s_m} - \frac{s_{m+1}}{q_m} \right) e^{iq_m \Delta z'_m} \right.$$
$$\left. + \left(1 - \frac{q_m}{s_m} - \frac{s_{m+1}}{s_m} + \frac{s_{m+1}}{q_m} \right) e^{-iq_m \Delta z'_m} \right], \tag{2.17}$$

915 A125-6

with $\hat{T}_{21} = \hat{T}_{12}^*$ and $\hat{T}_{22} = \hat{T}_{11}^*$. Here, the asterisk symbol represents the conjugate of a complex number.

2.1.1. *The three-layer case*

If we consider the special three-layer case (outgoing transmitted wave requires $a_2 = 0$), we can quickly obtain

$$\begin{bmatrix} a_1 \\ b_1 \end{bmatrix} = \begin{bmatrix} T_{11} & T_{12} \\ T_{21} & T_{22} \end{bmatrix} \begin{bmatrix} 0 \\ b_2 \end{bmatrix}, \tag{2.18}$$

where

$$\begin{bmatrix} T_{11} & T_{12} \\ T_{21} & T_{22} \end{bmatrix} = \boldsymbol{T}_{1,2}. \tag{2.19}$$

Thus we have

$$a_1 = T_{12}b_2, \tag{2.20}$$

$$a_2 = T_{22}b_2. \tag{2.21}$$

In Cai *et al.* (2021), we found that the averaged energy flux of a wave is

$$\langle F \rangle = \frac{C \text{Im}(\psi_z/\psi)}{2k^2\sigma}|\psi|^2, \tag{2.22}$$

where Im denotes the imaginary part of a complex number. Let us define the overall transmission ratio as

$$\eta = \frac{|\langle F \rangle_t|}{|\langle F \rangle_i|}, \tag{2.23}$$

where $\langle F \rangle_i$ is the averaged energy flux of the incident wave at the lowermost interface, and $\langle F \rangle_t$ is the averaged energy flux of the transmitted wave at the uppermost interface. For this three-layer case, we have

$$\eta = \left| \frac{s_2}{s_1} \right| \frac{|b_2|}{|a_2|} = \left| \frac{s_2}{s_1} \right| \frac{1}{|T_{22}|^2}. \tag{2.24}$$

From (2.16) and the relation between T_{22} and T_{11}, we obtain

$$|T_{22}|^2 = \frac{1}{4} \left[\left(1 + \frac{s_2}{s_1} \right)^2 \cos^2(q_1 \Delta z_1') + \left(\frac{q_1}{s_1} + \frac{s_2}{q_1} \right)^2 \sin^2(q_1 \Delta z_1') \right]$$

$$= \frac{1}{4} \left(1 + \frac{s_2}{s_1} \right)^2 \cos^2(q_1 \Delta z_1') + \frac{1}{4} \left(\frac{q_1}{s_1} + \frac{s_2}{q_1} \right)^2 \sin^2(q_1 \Delta z_1'). \tag{2.25}$$

Therefore, the overall transmission ratio is

$$\eta = \left[\frac{1}{4} \left(\sqrt{\frac{s_1}{s_2}} + \sqrt{\frac{s_2}{s_1}} \right)^2 \cos^2(q_1 \Delta z_1') + \frac{1}{4} \left(\sqrt{\frac{q_1^2}{s_1 s_2}} + \sqrt{\frac{s_1 s_2}{q_1^2}} \right)^2 \sin^2(q_1 \Delta z_1') \right]^{-1}. \tag{2.26}$$

Note that the terms inside square roots are always positive, no matter what direction of the propagating wave is. It is easy to prove $(\sqrt{s_1/s_2} + \sqrt{s_2/s_1})^2/4 \geq 1$, and so is the

term before $\sin^2(q_1 \Delta z_1')$. Thus, we can show $\eta \leq [\cos^2(q_1 \Delta z_1') + \sin^2(q_1 \Delta z_1')]^{-1} = 1$, which means that η is always smaller than or equal to 1. Gerkema & Exarchou (2008) have obtained a similar formula in their study on internal-wave transmission in weakly stratified layers. Their (38) is a special case of our formula (2.26) with $s_1 = s_2$. Some interesting conclusions can readily be drawn from (2.26). In the previous investigation of a two-layer structure (Wei 2020*a*; Cai *et al.* 2021), it has been found that wave transmission is hindered (because vertical wavelengths vary significantly across the interface) when the stable layer is strongly stratified ($N^2/(2\Omega)^2 \gg 1$). However, this is not always the case in the three-layer structure. For example, when $|q_1|\Delta z_1' \to \ell\pi$ (ℓ is a positive integer number) and $s_1/s_2 \to 1$, we see that $\eta \to 1$. For this case, there is no reflection and all of the incident wave is transmitted. This result is independent of $N^2/(2\Omega)^2$, and it holds for both weakly ($N^2/(2\Omega)^2 \ll 1$) and strongly ($N^2/(2\Omega)^2 \gg 1$) stratified rotating fluids. To better understand the behaviour of η, we separate η into two parts: the first part is the solution at $\sin^2(q_1 \Delta z_1') = 0$ and the second part is the solution at $\cos^2(q_1 \Delta z_1') = 0$. The transmission ratio η of the general case is a weighted harmonic mean of η_1 and η_2.

For the first part, the condition $\sin^2(q_1 \Delta z_1') = 0$ is equivalent to $\Delta z_1' = \ell\pi/|q_1|$. In other words, it requires that the thickness of the middle convective layer is a multiple of the half-wavelength of the propagating wave. In such a case, the overall transmission ratio is

$$\eta_1 = \left[\frac{1}{4} \left(\sqrt{\frac{s_1}{s_2}} + \sqrt{\frac{s_2}{s_1}} \right)^2 \right]^{-1}. \tag{2.27}$$

From this equation, we see that η_1 only depends on the wavenumber ratio s_2/s_1 of the stable layers. The value of η_1 decreases with s_2/s_1 when $s_2/s_1 > 1$, and increases with s_2/s_1 when $s_2/s_1 < 1$. The maximum value $\eta_1 = 1$ is achieved at $s_2/s_1 = 1$. Thus the transmission is efficient when $|N_1^2 - N_2^2|/(2\Omega)^2$ is small, or when the wave is at a critical colatitude $\theta_c = \cos^{-1} \pm\sigma/(2\Omega)$ (because $C \to 0$ when $\theta \to \theta_c$), or when both stable layers are weakly stratified (because $N_{1,2}^2 C \ll B^2 - A_0 C$). The latter two points have also been observed in the two-layer structure (Cai *et al.* 2021), while the first point is new to the three-layer structure. Enhancement of (near-inertial) wave transmission near the critical colatitude was also reported in Gerkema & Exarchou (2008) and André *et al.* (2017). Efficient wave transmission at critical colatitude and weakly stratified flow can be explained by a common reason: the inertial and gravity waves separated by an interface have almost the same vertical wavelengths, and thus these waves are 'resonant' at the interface. Similar reasoning can be used to explain the enhanced transmission when the degrees of stratification in both clamping layers (in configuration 1, the embedding convective layer is embedded within two neighbouring clamping stable layers) are similar: the incident wave is 'resonant', with waves in adjacent layers with wavelengths equal to free modes of the multi-layer structure (André *et al.* 2017).

Figure 3 shows the transmission ratio η_1 at three different combinations of N_1^2 and N_2^2. In figure 3(*a*–*c*), both stable layers are strongly stratified, but $N_1^2/(2\Omega)^2$ is equal to $N_2^2/(2\Omega)^2$. This clearly shows that the transmission is enhanced. Figure 3(*d*–*f*) shows the result of the cases with one weakly and one strongly stratified layer. Apparently, the transmission is not as efficient as the cases shown panels (*a,b,c*). Figure 3(*g*–*i*) presents the result of the cases with two weakly stratified stable layers. The transmission is efficient because the rotational effect is important. In a previous study on wave transmission in a two-layer structure (Cai *et al.* 2021), it has been shown that a wave can be efficiently transmitted when the stable layer is weakly stratified. From figure 3, we also observe
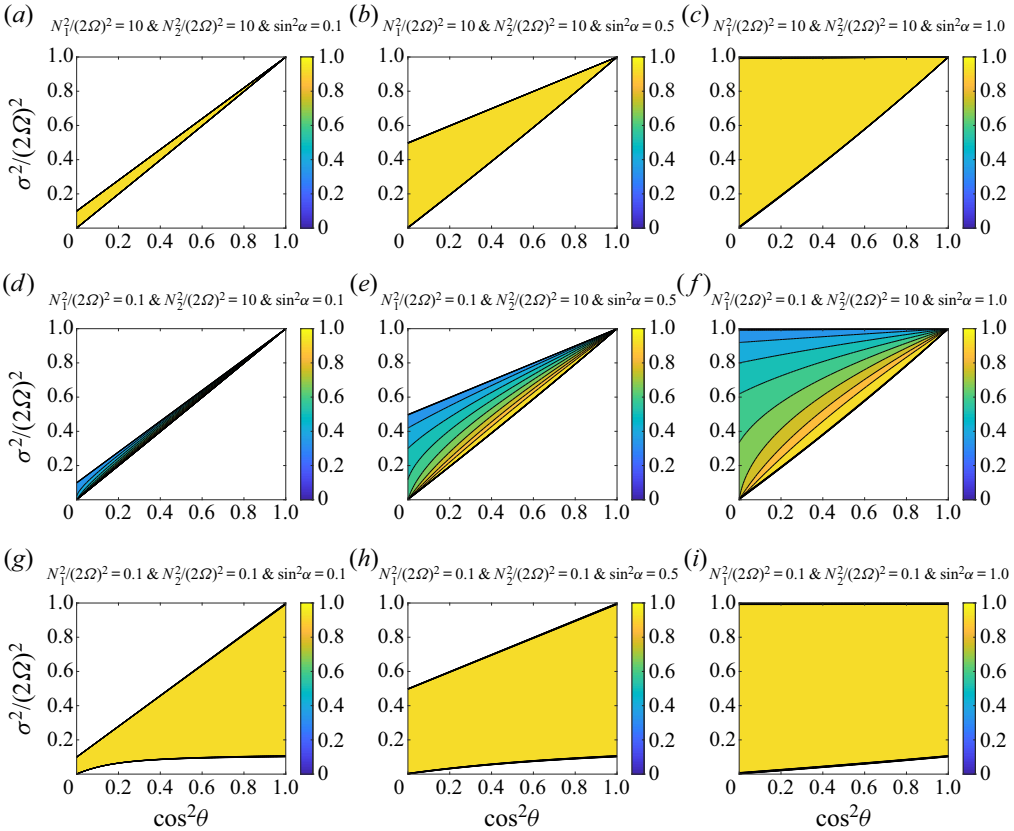
Figure 3. Transmission coefficient η_1 (the first part of (2.26)) for different $N_{1,2}^2/(2\Omega)^2$ and $\sin^2\alpha$ in a three-layer structure (one middle convective layer and two upper and lower neighbouring stable layers). The horizontal axis is $\cos^2\theta$, and the vertical axis is $\sigma^2/(2\Omega)^2$. From the left to the right panels, $\sin^2\alpha$ increases from 0.1 to 1.0. (*a–c*) Both stable layers are strongly stratified. (*d–f*) One stable layer is strongly stratified and the other is weakly stratified. (*g–i*) Both stable layers are weakly stratified. Wave propagation can only occur in coloured regions. Regions are left white if wave propagation is prohibited.

that $\sin^2\alpha$ has important effect on the frequency range. Frequency range increases with increasing $\sin^2\alpha$. When stable layers (or any of them) are strongly stratified, a wave can only survive in a very thin region if $\sin^2\alpha$ is small. In the extreme case $\sin^2\alpha = 0$, the surviving frequency range vanishes.

For the second part, the condition $\cos^2(q_1\Delta z_1') = 0$ is equivalent to $\Delta z_1' = (\ell + 1/2)\pi/|q_1|$, which requires that the thickness of the middle convective layer is a multiple-and-a-half of the half-wavelength of the propagating wave. In such a case, the overall transmission ratio is

$$\eta_2 = \left[\frac{1}{4}\left(\sqrt{\frac{q_1^2}{s_1 s_2}} + \sqrt{\frac{s_1 s_2}{q_1^2}}\right)^2\right]^{-1}. \tag{2.28}$$

Similarly, η_2 only depends on the wavenumber ratio $s_1 s_2/q_1^2$. It decreases with $s_1 s_2/q_1^2$ when $s_1 s_2/q_1^2 > 1$ and increases with $s_1 s_2/q_1^2$ when $s_1 s_2/q_1^2 < 1$. Let us consider two cases $C > 0$ and $C < 0$. For the first case we have $|s_{1,2}| < |q_1|$, while for the second case
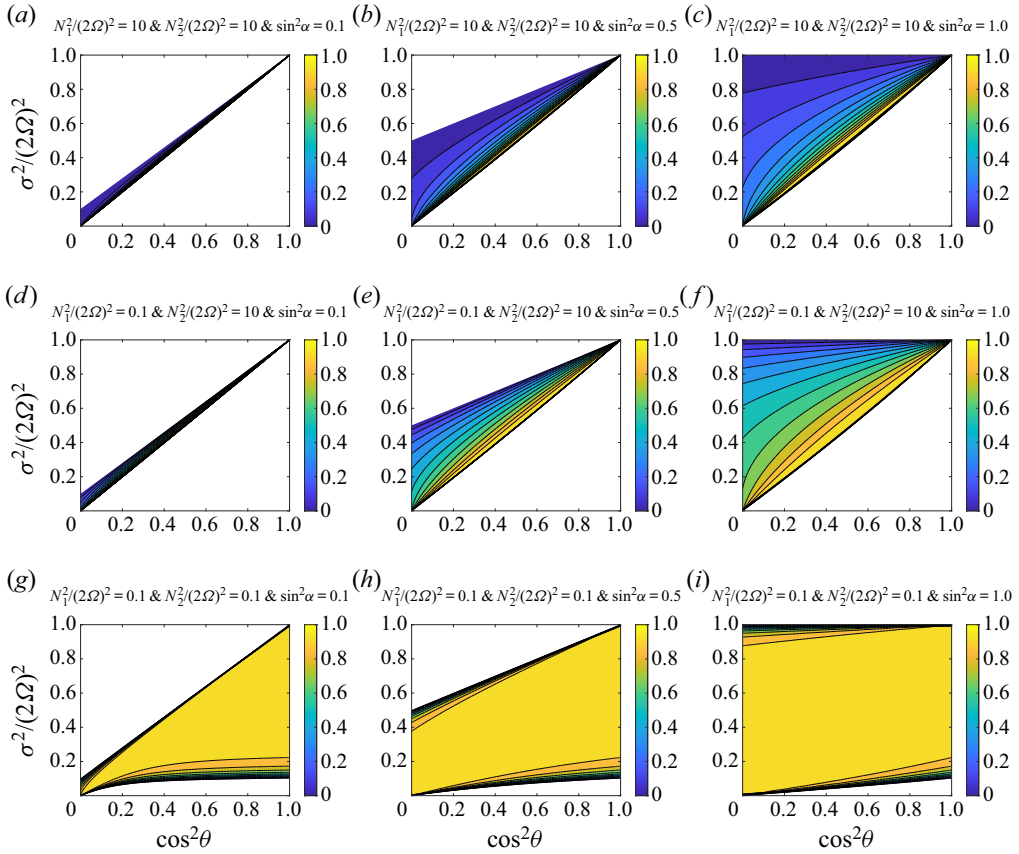
915 A125-9

Figure 4. Transmission coefficient η_2 (the second part of (2.26)) for different $N_{1,2}^2/(2\Omega)^2$ and $\sin^2\alpha$ in a three-layer structure (one middle convective layer and two upper and lower neighbouring stable layers). The horizontal axis is $\cos^2\theta$, and the vertical axis is $\sigma^2/(2\Omega)^2$. From the left to the right panels, $\sin^2\alpha^2$ increases from 0.1 to 1.0. (a–c) Both stable layers are strongly stratified. (d–f) One stable layer is strongly stratified and the other is weakly stratified. (g–i) Both stable layers are weakly stratified. Wave propagation can only occur in coloured regions. Regions are left white if wave propagation is prohibited.

we have $|s_{1,2}| > |q_1|$. Thus, for $C > 0$, we obtain $s_1 s_2 / q_2^2 < 1$ and η_2 always increases with $s_1 s_2 / q_1^2$. While for the other case, $C < 0$, we obtain $s_1 s_2 / q_2^2 > 1$ and η_2 always decreases with $s_1 s_2 / q_1^2$. Efficient transmission can occur if $s_1 s_2 / q_1^2 \to 1$, which basically requires both $N_1^2 C/(B^2 - A_0 C)$ and $N_2^2 C/(B^2 - A_0 C)$ to be small. This indicates that the transmission ratio will decrease if both $N_1^2/(2\Omega)^2$ and $N_2^2/(2\Omega)^2$ increase, no matter what the sign of C is. Figure 4 gives an example of such case. Apparently, it can be seen that the transmission ratio decreases when the stable layers are varied from weakly stratified (g,h,i) to strongly stratified (a,b,c). Also apparent is that transmission is efficient near the critical colatitudes, where $N_{1,2}^2 C/(B^2 - A_0 C) \to 0$.

Although the deduced transmission ratio (2.26) is for configuration 1, it can be generalized to other configurations. For configuration 2 (figure 2b), the stable layer is embedded between two convective layers. We label the stable layer as $m + 1/2$, and the neighbouring convective layers as m and $m + 1$. The neighbouring upper and lower interfaces of the stable layer $m + 1/2$ are at z_m and z'_m. In this setting, the transmission

915 A125-10

ratio can be deduced by simply interchanging q_m with s_m in (2.26). Therefore, we obtain the overall transmission ratio in configuration 2 as

$$\eta = \left[\frac{1}{4}\left(\sqrt{\frac{q_1}{q_2}} + \sqrt{\frac{q_2}{q_1}}\right)^2 \cos^2(s_1\Delta z_1') + \frac{1}{4}\left(\sqrt{\frac{s_1^2}{q_1 q_2}} + \sqrt{\frac{q_1 q_2}{s_1^2}}\right)^2 \sin^2(s_1\Delta z_1')\right]^{-1}.$$

(2.29)

The wavenumbers in the convective layers are all the same, thus we have

$$\eta = \left[\cos^2(s_1\Delta z_1') + \frac{1}{4}\left(\left|\frac{s_1}{q_1}\right| + \left|\frac{q_1}{s_1}\right|\right)^2 \sin^2(s_1\Delta z_1')\right]^{-1}.$$

(2.30)

Again, we can show that wave transmission is enhanced when the thickness of the middle stable layer is a multiple of the half-wavelength of the propagating wave.

2.1.2. *The multiple-layer case*

Now we consider the structure with more alternating layers. Here, we first discuss the case of $2M + 1$ alternating layers ($M + 1$ stable layers and M convective layers), and both the lowermost and uppermost layers are stable. From the recursive relation (2.15), we have

$$\begin{bmatrix} a_1 \\ b_1 \end{bmatrix} = \prod_{m=1}^{M} \boldsymbol{T}_{m,m+1} \begin{bmatrix} a_{M+1} \\ b_{M+1} \end{bmatrix} = \begin{bmatrix} T_{11} & T_{12} \\ T_{21} & T_{22} \end{bmatrix} \begin{bmatrix} a_{M+1} \\ b_{M+1} \end{bmatrix}.$$

(2.31)

Letting $a_{M+1} = 0$, we obtain that the wave amplitude of the transmitted wave in the uppermost layer is $b_{M+1} = T_{22}^{-1}b_1$, and the transmission ratio is

$$\eta = \left|\frac{s_{M+1}}{s_1}\right| \frac{1}{|T_{22}|^2}.$$

(2.32)

Now we discuss the case of $2M$ alternating layers (M stable layers and M convective layers), and the lowermost layer is stable and the uppermost layer is convective. Using the recursive relation (2.15) and combining it with the boundary conditions at the uppermost interface, we have

$$\begin{bmatrix} a_1 \\ b_1 \end{bmatrix} = \left(\prod_{m=1}^{M-1} \boldsymbol{T}_{m,m+1}\right) S_M^{-1} \Lambda_{M,M} Q_{M,M} \begin{bmatrix} c_M \\ d_M \end{bmatrix} = \begin{bmatrix} T_{11}' & T_{12}' \\ T_{21}' & T_{22}' \end{bmatrix} \begin{bmatrix} c_M \\ d_M \end{bmatrix},$$

(2.33)

where T_{ij}', $i, j \in \{1, 2\}$ is defined by the matrix multiplications shown in the middle of (2.33). Letting $c_M = 0$, we obtain that the wave amplitude of the transmitted wave in the uppermost layer is $d_{M+1} = T_{22}'b_1$, and the transmission ratio is

$$\eta = \left|\frac{q_M}{s_1}\right| \frac{1}{|T_{22}'|^2}.$$

(2.34)

Again, following similar procedures, we can deduce the transmission ratio of configuration 2 by interchanging q_m with s_m.

We have shown that the transmission can be enhanced in the three-layer structure of configuration 1. Now we investigate whether the enhancement occurs in a structure with

more layers. For the sake of simplicity, we assume that all convective layers have the same thickness Δz_c and wavenumber q, and all stable layers have the same thickness Δz_s and wavenumber s.

We first discuss the case when the number of layers $(2M + 1)$ is odd. When $s_m = s$, $q_m = q$ and $\Delta z'_m = \Delta z_c$, the transfer matrix $\boldsymbol{T}_{m,m+1} = T$ is

$$\hat{T}_{11} = \frac{1}{4} e^{-is\Delta z_c} \left\{ \left[2 + \left(\frac{q}{s} + \frac{s}{q} \right) \right] e^{iq\Delta z_c} + \left[2 - \left(\frac{q}{s} + \frac{s}{q} \right) \right] e^{-iq\Delta z_c} \right\}, \quad (2.35)$$

$$\hat{T}_{12} = \frac{1}{4} e^{i(sz_m + sz'_m)} \left[\left(\frac{q}{s} - \frac{s}{q} \right) e^{iq\Delta z_c} - \left(\frac{q}{s} - \frac{s}{q} \right) e^{-iq\Delta z_c} \right], \quad (2.36)$$

with $\hat{T}_{22} = \hat{T}_{11}^*$ and $\hat{T}_{21} = \hat{T}_{12}^*$. The eigenvalue satisfies the following equation:

$$(\hat{T}_{11} - \lambda)(\hat{T}_{22} - \lambda) = \hat{T}_{12}\hat{T}_{21}. \quad (2.37)$$

After some manipulations, the equation can be written as

$$\lambda^2 - 2\text{Re}(\hat{T}_{11})\lambda + 1 = 0, \quad (2.38)$$

or in an explicit form

$$\lambda^2 - 2 \left[\cos(q\Delta z_c) \cos(s\Delta z_c) + \frac{1}{2} \left(\frac{q}{s} + \frac{s}{q} \right) \sin(q\Delta z_c) \sin(s\Delta z_c) \right] \lambda + 1 = 0, \quad (2.39)$$

where Re denotes the real part of a complex number. Let $\lambda_{1,2}$ be the two roots of the equation. Obviously, we have $\lambda_1 \lambda_2 = 1$. Let

$$\Delta_\lambda = \left[\cos(q\Delta z_c) \cos(s\Delta z_c) + \frac{1}{2} \left(\frac{q}{s} + \frac{s}{q} \right) \sin(q\Delta z_c) \sin(s\Delta z_c) \right]^2 - 1 \quad (2.40)$$

$$= \left\{ \cos[(q - s)\Delta z_c] + \frac{1}{2} \left(\frac{q}{s} + \frac{s}{q} - 2 \right) \sin(q\Delta z_c) \sin(s\Delta z_c) \right\}^2 - 1. \quad (2.41)$$

Then, the eigenvalues $\lambda_{1,2}$ are real when $\Delta_\lambda > 0$, and are complex when $\Delta_\lambda < 0$. If $\lambda_{1,2}$ are real and $\lambda_1 \neq \lambda_2$, then the maximum of $|\lambda_{1,2}|$ must be greater than one. For a multi-layer structure, the transfer matrix $\boldsymbol{T}^M \propto \max(|\lambda_{1,2}|)^M$, which yields $\eta \propto \max(|\lambda_{1,2}|)^{-M}$. Since $\max(|\lambda_{1,2}|)$ is greater than one, the transmission ratio decays with the number of layers.

To ensure that the transmission does not decay, the solution $\lambda_{1,2}$ must be on the unit circle of the complex plane. This condition can be achieved when $\lambda_1 = \lambda_2 = \pm 1$, or $\lambda_{1,2}$ are a complex pair. Therefore, a necessary condition (not sufficient) for efficient wave transmission is $\Delta_\lambda \leq 0$.

It should be emphasized that the condition $\Delta_\lambda \leq 0$ is not a sufficient condition. The transmission ratio is actually determined by $|T_{22}|$, which could possibly be much greater than one even though the eigenvalues $\lambda_{1,2}$ are on the unit circle. Here, we take a further step to discuss when the value $|T_{22}|$ will be close to one, so as to ensure an efficient wave transmission.

Let us further define $z = 0$ at the lowest interface, and $\alpha_1 = \exp(-is\Delta z_s)$ and $\alpha_2 = \exp(-is\Delta z_c)$. With such definitions, we have $z_m + z'_m = (2m - 2)\Delta z_s + (2m - 1)\Delta z_c$ and

915 A125-12

$\exp[-\mathrm{i}s(z_m + z'_m)] = \alpha_1^{2m-2}\alpha_2^{2m-1}$. The transfer matrix can be rewritten as

$$\boldsymbol{T}_{m,m+1} = \begin{bmatrix} \alpha_2 \tilde{T}_{11} & \alpha_1^{*2m-2}\alpha_2^{*2m-1}\tilde{T}_{12} \\ \alpha_1^{2m-2}\alpha_2^{2m-1}\tilde{T}_{12}^* & \alpha_2^*\tilde{T}_{11}^* \end{bmatrix}, \tag{2.42}$$

where

$$\tilde{T}_{11} = \frac{1}{4}\left\{\left[2 + \left(\frac{q}{s} + \frac{s}{q}\right)\right] \mathrm{e}^{\mathrm{i}q\Delta z_c} + \left[2 - \left(\frac{q}{s} + \frac{s}{q}\right)\right] \mathrm{e}^{-\mathrm{i}q\Delta z_c}\right\}, \tag{2.43}$$

$$\tilde{T}_{12} = \frac{1}{4}\left[\left(\frac{q}{s} - \frac{s}{q}\right) \mathrm{e}^{\mathrm{i}q\Delta z_c} - \left(\frac{q}{s} - \frac{s}{q}\right) \mathrm{e}^{-\mathrm{i}q\Delta z_c}\right]. \tag{2.44}$$

When $m = 1$, we note that the transfer matrix $\boldsymbol{T}_{1,2}$ can be formulated as

$$\boldsymbol{T}_{1,2} = \begin{bmatrix} \alpha_2 \tilde{T}_{11} & \alpha_2^*\tilde{T}_{12} \\ \alpha_2 \tilde{T}_{12}^* & \alpha_2^*\tilde{T}_{11}^* \end{bmatrix} = \boldsymbol{A}\begin{bmatrix} \alpha_2 & 0 \\ 0 & \alpha_2^* \end{bmatrix}, \tag{2.45}$$

where

$$\boldsymbol{A} = \begin{bmatrix} \tilde{T}_{11} & \tilde{T}_{12} \\ \tilde{T}_{12}^* & \tilde{T}_{11}^* \end{bmatrix}. \tag{2.46}$$

Here, we consider a special case with $\alpha_1^2 = \alpha_1^{*2} = 1$, which can be achieved by letting $|s|\Delta z_s = \ell'\pi$, where ℓ' is a non-negative integer. For this special case, it can be proved that

$$\prod_{m=1}^{M} \boldsymbol{T}_{m,m+1} = \boldsymbol{A}^M \begin{bmatrix} \alpha_2^M & 0 \\ 0 & \alpha_2^{*M} \end{bmatrix}. \tag{2.47}$$

Now we try to derive the explicit form of $\boldsymbol{A}^M$. It is obvious that $\tilde{T}_{12}$ is a pure imaginary number, thus we can write $\boldsymbol{A}$ as

$$\boldsymbol{A} = \begin{bmatrix} \mathrm{Re}(\tilde{T}_{11}) + \mathrm{i}\mathrm{Im}(\tilde{T}_{11}) & \mathrm{i}\mathrm{Im}(\tilde{T}_{12}) \\ -\mathrm{i}\mathrm{Im}(\tilde{T}_{12}) & \mathrm{Re}(\tilde{T}_{11}) - \mathrm{i}\mathrm{Im}(\tilde{T}_{11}) \end{bmatrix} = \cos(q\Delta z_c)\boldsymbol{I} + \mathrm{i}\boldsymbol{U}, \tag{2.48}$$

where

$$\boldsymbol{U} = \begin{bmatrix} \mathrm{Im}(\tilde{T}_{11}) & \mathrm{Im}(\tilde{T}_{12}) \\ -\mathrm{Im}(\tilde{T}_{12}) & -\mathrm{Im}(\tilde{T}_{11}) \end{bmatrix}, \tag{2.49}$$

and it is easy to verify

$$\boldsymbol{U}^2 = \sin^2(q\Delta z_c)\boldsymbol{I}. \tag{2.50}$$

If $\sin(q\Delta z_c) = 0$, we can show $\boldsymbol{A} = \cos(q\Delta z_c)\boldsymbol{I}$ and $\boldsymbol{A}^M = \cos^M(q\Delta z_c)\boldsymbol{I}$. If $\sin(q\Delta z_c) \neq 0$, then we obtain

$$\boldsymbol{A}^M = (\cos(q\Delta z_c)\boldsymbol{I} + \mathrm{i}\boldsymbol{U})^M \tag{2.51}$$

$$= \boldsymbol{I} \sum_{k \in even} C_k^M \cos^{M-k}(q\Delta z_c)\mathrm{i}^k \sin^k(q\Delta z_c)$$

$$+ \boldsymbol{U}[\sin(q\Delta z_c)]^{-1} \sum_{k \in odd} C_k^M \cos^{M-k}(q\Delta z_c)\mathrm{i}^k \sin^k(q\Delta z_c) \tag{2.52}$$

$$= \cos(Mq\Delta z_c)\boldsymbol{I} + \mathrm{i}\sin(Mq\Delta z_c)[\sin(q\Delta z_c)]^{-1}\boldsymbol{U}, \tag{2.53}$$

915 A125-13

where $C_k^M = M!/((M - k)!k!)$ is the combination function. From the above calculation, the analytical solution of the transmission ratio can be obtained. If $\sin(q\Delta z_c) = 0$, we have

$$T_{22} = \alpha_2^{*M} \cos^M(q\Delta z_c), \qquad (2.54)$$

and the transmission ratio is

$$\eta = 1. \qquad (2.55)$$

If $\sin(q\Delta z_c) \neq 0$, we have

$$T_{22} = \alpha_2^{*M} \left[\cos(Mq\Delta z_c) - \mathrm{i}\frac{1}{2}\left(\frac{q}{s} + \frac{s}{q}\right) \sin(Mq\Delta z_c) \right], \qquad (2.56)$$

and the transmission ratio is

$$\eta = \left[\cos^2(Mq\Delta z_c) + \frac{1}{4}\left(\frac{q}{s} + \frac{s}{q}\right)^2 \sin^2(Mq\Delta z_c) \right]^{-1}. \qquad (2.57)$$

Equation (2.55) can be synthesized into (2.57), since $\sin(q\Delta z_c) = 0$ implies $\sin^2(Mq\Delta z_c) = 0$ and $\cos^2(Mq\Delta z_c) = 1$. Therefore, we conclude that, under the condition $|s|\Delta z_s = \ell'\pi$, the wave transmission ratio can be described by (2.57). Comparing with the result of three-layer structure case, we see that (2.26) is just a special case of (2.57) when $M = 1$. The discussion on efficiency of wave transmission based on (2.57) is similar to that in three-layer structure case, and here we will not repeat it. From the analytical solution, it is clear that the wave will be totally transmitted when $M|q|\Delta z_c = \ell\pi$ and $|s|\Delta z_s = \ell'\pi$.

Analytical solution of the general cases of $|s|\Delta z_s \neq \ell'\pi$ is more difficult, but some insights can be provided from the discussion of the eigenvalues of the transmission matrix. It is worth mentioning that, for the special case when $\sin q\Delta z_c \to 0$ and $\sin s\Delta z_c \to 0$, the eigenvalues $|\lambda_{1,2}| \to 1$. In this limit, it can be shown that

$$\Delta_\lambda \sim \frac{[mod((q - s)\Delta z_c, \pi)]^4}{12} > 0, \qquad (2.58)$$

where *mod* is the modulo function. The eigenvalues are real numbers, and one of $|\lambda_{1,2}|$ is slightly greater than 1. The transmission decays slowly as the wave crosses each layer. The wave transmission can be efficient when the number of layers is not too large. The eigenvalues can be estimated as

$$\lambda_{1,2} = \sqrt{1 + \Delta_\lambda} \pm \sqrt{\Delta_\lambda} \sim 1 \pm \frac{[mod((q - s)\Delta z_c, \pi)]^2}{3\sqrt{2}}. \qquad (2.59)$$

Thus, the decay rate of the transmission ratio is approximately $\lambda_2^{-M} \sim \{1 - 12^{-1/2}M[mod((q - s)\Delta z_c, \pi)]^2\}^{-1}$. The transmission can be efficient when $M \ll M_c = [mod((q - s)\Delta z_c, \pi)]^{-2}$. When $mod((q - s)\Delta z_c, \pi) \to 0$, the critical value M_c is very large. As a result, the transmission can be approximately efficient in this case. From the above discussion, we infer that the transmission can be efficient when $\sin(q\Delta z_c) \ll 1$ or $\sin(s\Delta z_c) \ll 1$. This conclusion is useful when embedded convective layers are very thin.

When the total number of layers is even $(2M)$, we can consider the case as one of $(2M - 1)$ layers plus an additional layer. The best scenario for transmission for $(2M - 1)$ layers is that the incident wave is totally transmitted to the $(2M - 1)$th layer. Now the wave is incident from the $(2M - 1)$th layer to the $(2M)$th layer, and it can be considered as a
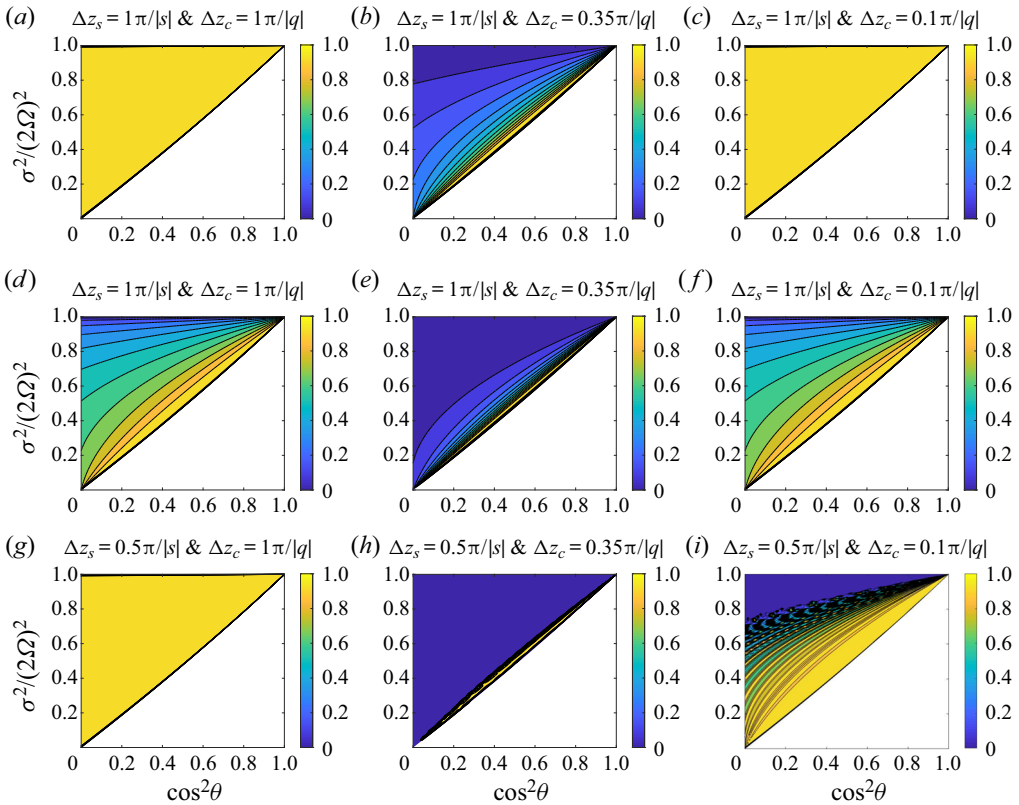
Figure 5. Transmission ratios in multi-layer structures. For all the cases, $N_m^2/(2\Omega)^2 = 10$ and $\sin^2\alpha = 1$, and the lowermost layer is stable; $\Delta z_s = \pi/|s|$ for $(a\text{--}f)$ but $\Delta z_s = 0.5\pi/|s|$ for $(g\text{--}i)$. In each case, all the convective layers have the same thickness Δz_c and wavenumber q, and all the stable layers have the same thickness Δz_s and wavenumber s. $(a\text{--}c)$ The transmission ratio for a 101-layer structure with $\Delta z_c = (1, 0.35, 0.1)\pi/|q|$. $(d\text{--}f)$ The transmission ratio for a 102-layer structure with $\Delta z_c = (1, 0.35, 0.1)\pi/|q|$. $(g\text{--}i)$ Similar to $(a\text{--}c)$ but with different Δz_s. Wave propagation can only occur in coloured regions. Regions are left white if wave propagation is prohibited.

two-layer problem. For a two-layer problem, wave transmission is generally not efficient when the stable layer is strongly stratified (Wei 2020*a*; Cai *et al.* 2021).

Figure 5 plots the transmission ratios in a 101-layer structure (a,b,c) and a 102-layer structure (d,e,f). In all the cases, we choose $N_m^2/(2\Omega)^2 = 10$, $\sin^2\alpha = 1$ and the lowermost layer is stable. Thus, in all cases, the stable layers are strongly stratified. This clearly shows that the transmission is enhanced in figure 5(a,c), where the total number of layers is odd and Δz_c and Δz_s satisfy the conditions $M|q|\Delta z_c = \ell\pi$ and $|s|\Delta z_s = \ell'\pi$. The transmission in figure 5(b) is not enhanced because $M|q|\Delta z_c \neq \ell\pi$. For the case of 102-layer structure (figure 5d,f), the transmission is not enhanced even when the above conditions are satisfied. For these two cases, the wave is almost totally transmitted from the first layer to 101st layer (see figure 5a,c). Wave transmission from the 101st layer to 102nd layer can be viewed as a two-layer problem, and it is generally not efficient when the stable layer is strongly stratified. Therefore, if the stable layer is strongly stratified, the enhancement of transmission only takes place when the number of alternating layers is odd. In other words, enhanced wave transmission only occurs in a multi-layer structure with stable layers embedded within convective layers, or convective layers embedded
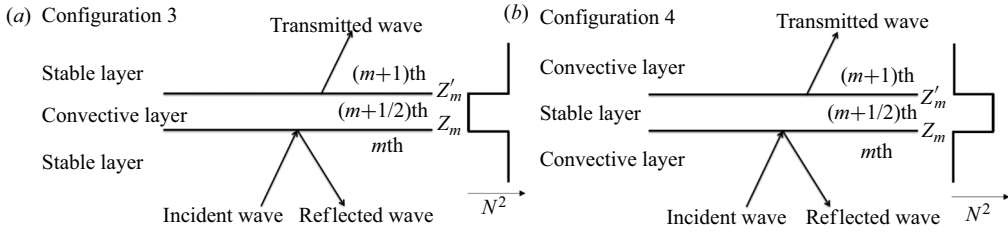
Figure 6. Two configurations of tunnelling of gravity and inertial waves. (*a*) Tunnelling of a gravity wave. Both top and bottom layers are stable. Gravity wave can propagate in the stable layer, but wave cannot propagate in the convective layer. (*b*) Tunnelling of an inertial wave. Both top and bottom layers are convective. Gravity wave can propagate in the convective layer, but wave cannot propagate in the stable layer.

within stable layers. The enhancement of transmission also depends on the thicknesses of embedded layers Δz_s. Figure 5(*g–i*) presents results of three cases with $|s|\Delta z_s = 0.5\pi$ and different values of $|q|\Delta z_c$. It can be seen that the transmission of the case $|q|\Delta z_c = \pi$ is enhanced, while the transmission of the case $|q|\Delta z_c = 0.1\pi$ is only partially enhanced.

The result obtained in the configuration 1 is also true in the configuration 2. Here, we do not repeat the discussion on configuration 2. André *et al.* (2017) have also observed that wave transmission can be enhanced in a multi-layer structure. They provided a physical explanation for the enhancement in wave transmission when the incident wave is resonant with waves in adjacent layers with half-wavelengths equal to the layer depth. Our analysis verifies this phenomenon from a mathematical point of view.

2.2. *Wave tunnelling*

In the previous section, we have considered wave transmissions in multiple convective and radiative (stable) layers when the condition $B^2 - AC > 0$ is satisfied everywhere in the domain. Here, we consider wave transmissions in two other configurations: (i) wave solution exists in stable layers but not in convective layers; (ii) wave solution exists in convective layers but not in stable layers. For the first configuration, a gravity wave can propagate in stable layers; and for the second configuration, an inertial wave can propagate in convective layers. Figure 6 shows the plots of a three-layer structure for the two configurations. In figure 6(*a*), the convective layer is embedded within two stable layers. In figure 6(*b*), the stable layer is embedded within two convective layers. For multiple layer structures in figure 6, although the wave cannot propagate in the whole domain, it still can transmit through a tunnelling process (Sutherland & Yewchuk 2004; Mihalas & Mihalas 2013). In the following, we will discuss the tunnelling of gravity and inertial waves, respectively.

2.2.1. *Tunnelling of gravity waves*

For configuration 3 in figure 6(*a*), the wave can propagate in the stable layer but cannot propagate in the convective layer. Thus the wave frequency must be in the range $\sigma_4^2 < \sigma^2 < \sigma_5^2$. The width of the frequency domain can be written as

$$\sigma_5^2 - \sigma_4^2 = \frac{1}{2}\left[(N_{min}^2 - f^2 - \tilde{f}_s^2) + \sqrt{(N_{min}^2 - f^2 - \tilde{f}_s^2)^2 + 4N_{min}^2\tilde{f}_s^2} \right]. \qquad (2.60)$$

For the sake of convenience, we only discuss waves at the northern hemisphere ($\theta \in [0, \pi/2]$). The result at the southern hemisphere can be inferred from the

symmetry property. From (2.60), it can be proved that $\sigma_5^2 - \sigma_4^2$ always increases with θ, $\sin^2 \alpha$, and $N_{min}^2/(2\Omega)^2$ (see Appendix B). Therefore, the frequency domain is wider at the equatorial regions than at the polar regions. Also, it is wider when the meridional wavenumber dominates the zonal wavenumber, and it is wider when the degree of stratification is stronger.

Now we discuss the wave tunnelling in configuration 3. We use the same setting as that discussed in wave propagation. The derivation of wave transmission by tunnelling is similar to that of wave propagation. The only difference is that now the wave cannot propagate in the convective layer, and thus $q_m = i\hat{q}_m$ is a pure imaginary number. Then the transfer relation from the mth layer to the $(m + 1)$th layer can be easily obtained by replacing q_m with $i\hat{q}_m$ in (2.15).

Replacing q_m with $i\hat{q}_m$ in (2.15), we can obtain the transfer matrix. In this configuration, we always have $C = f^2 - \sigma^2 < 0$ (since $\sigma_4^2 > f^2$). Hence, for an outgoing transmitted wave, we have $b_{M+1} = 0$ (modified phase velocity has an opposite sign to the group velocity). Again, let us first discuss the transmission ratio for a three-layer structure. In such a case, we have $a_1 = T_{11}a_2$ and

$$T_{11} = \frac{1}{4} \, e^{-i(s_1 z_1 - s_2 z_1')} \left[(1 + \frac{i\hat{q}_1}{s_1} + \frac{s_2}{s_1} + \frac{s_2}{i\hat{q}_1}) \, e^{-\hat{q}_1 \Delta z_1'} + (1 - \frac{i\hat{q}_1}{s_1} + \frac{s_2}{s_1} - \frac{s_2}{i\hat{q}_1}) \, e^{\hat{q}_1 \Delta z_1'} \right]. \tag{2.61}$$

Thus the wave transmission ratio is

$$\eta = \left| \frac{s_2}{s_1} \right| \frac{1}{|T_{11}|^2} \tag{2.62}$$

$$= 16 \left[\left(\sqrt{\frac{s_1}{s_2}} + \sqrt{\frac{s_2}{s_1}} \right)^2 (e^{-\hat{q}_1 \Delta z_1'} + e^{\hat{q}_1 \Delta z_1'})^2 \right.$$

$$\left. + \left(\sqrt{\frac{\hat{q}_1^2}{s_1 s_2}} - \sqrt{\frac{s_1 s_2}{\hat{q}_1^2}} \right)^2 (e^{-\hat{q}_1 \Delta z_1'} - e^{\hat{q}_1 \Delta z_1'})^2 \right]^{-1} \tag{2.63}$$

$$= 16 \left\{ \left(\sqrt{\frac{s_1}{s_2}} + \sqrt{\frac{s_2}{s_1}} \right)^2 (e^{-\hat{q}_1 \Delta z_1'} + e^{\hat{q}_1 \Delta z_1'})^2 \right.$$

$$\left. + \left[\left(\sqrt{\frac{\hat{q}_1^2}{s_1 s_2}} + \sqrt{\frac{s_1 s_2}{\hat{q}_1^2}} \right)^2 - 4 \right] [(e^{-\hat{q}_1 \Delta z_1'} + e^{\hat{q}_1 \Delta z_1'})^2 - 4] \right\}^{-1}. \tag{2.64}$$

Obviously, η depends on the values of s_1/s_2, $\hat{q}_1^2/(s_1 s_2)$ and $|\hat{q}_1|\Delta z_1'$. It increases with s_1/s_2 when $s_1/s_2 < 1$, and decreases with s_1/s_2 when $s_1/s_2 > 1$. Similarly, we see that it increases with $\hat{q}_1^2/(s_1 s_2)$ when $\hat{q}_1^2/(s_1 s_2) < 1$, and decreases with $\hat{q}_1^2/(s_1 s_2)$ when $\hat{q}_1^2/(s_1 s_2) > 1$. It is also noted that it decreases with $|\hat{q}_1|\Delta z_1'$. Thus, an efficient transmission ratio can be achieved when $s_1 \to s_2$, $\hat{q}_1^2 \to s_1 s_2$ and $|\widehat{q_1}|\Delta z_1' \to 0$. The condition $\hat{q}_1^2 \to s_1 s_2$ can be relaxed if $|\widehat{q_1}|\Delta z_1' \to 0$. Therefore, efficient transmission requires that the wavenumbers (s_1 and s_2) in the stable layers are similar in magnitude,
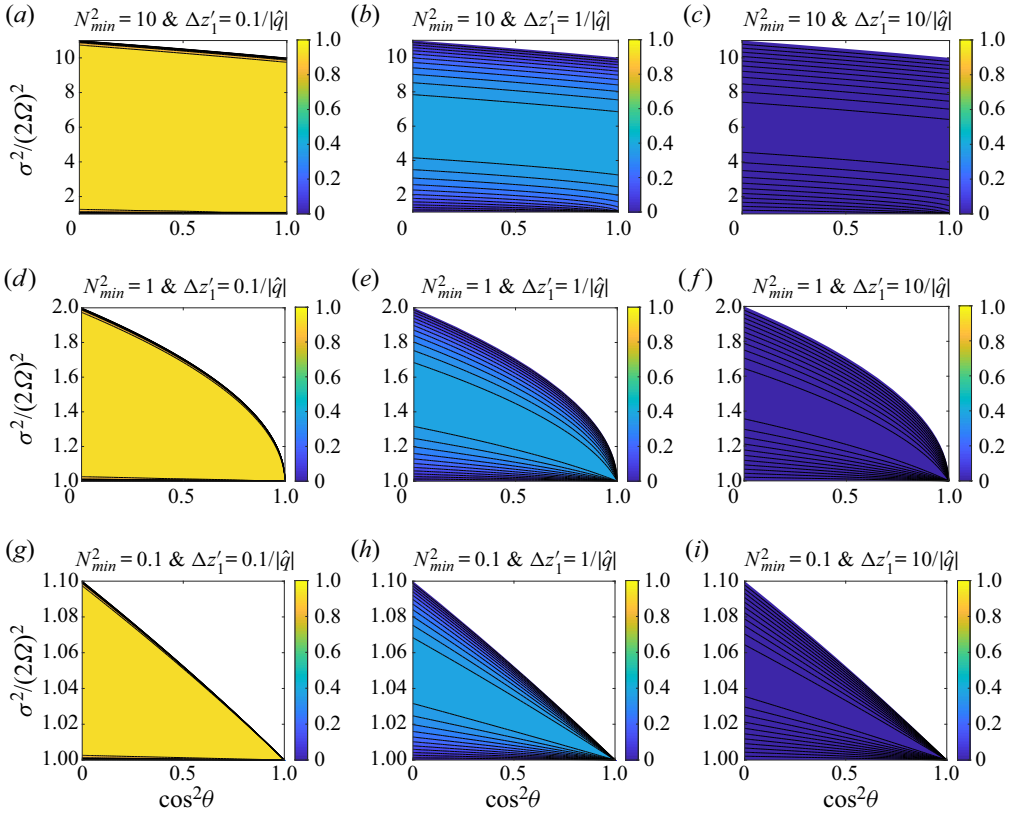
Figure 7. Contour plots of transmission ratios for the tunnelling of a gravity wave in a three-layer structure. (a–c) Transmission ratios when the buoyancy frequency $N_{min}^2 = 10$, and $\Delta z_1' = (0.1, 1, 10)/|\hat{q}_1|$. ($d$–$f$) Transmission ratios when the buoyancy frequency $N_{min}^2 = 1$, and $\Delta z_1' = (0.1, 1, 10)/|\hat{q}_1|$. ($g$–$i$) Transmission ratios when the buoyancy frequency $N_{min}^2 = 0.1$, and $\Delta z_1' = (0.1, 1, 10)/|\hat{q}_1|$. tunnelling of gravity waves can only occur in coloured regions. Regions are left white if tunnelling of gravity waves is prohibited.

and the thickness of the convective layer ($\Delta z_1'$) is much smaller than the e-folding decay distance ($1/|\hat{q}_1|$). Figure 7 shows contour plots of the transmission ratios for different N_{min}^2 and $\Delta z_1'$. In all cases, we set $s_1 = s_2$ and $\sin^2 \alpha = 1$. First, the figure clearly shows that the frequency domain increases with N_{min}^2 and θ. This is consistent with the previous analysis on the width of the frequency domain. Second, we see that the transmission ratio is mainly affected by the thickness of the convective layer $\Delta z_1'$. The shallower the convective layer is, the higher the transmission ratio is. We also note that the transmission ratio is insensitive to N_{min}^2. The effect of degree of stratification on the transmission ratio is insignificant.

Now we consider the wave transmission in configuration 3 with more layers. Again, we assume that all of the stable layers have the same degree of stratification (N_1^2) and thickness (Δz_s). Similarly, we assume that all of the convective layers have the same thickness Δz_c. With these conditions, $s_m = s$ and $q_m = i\hat{q}$ are constants in the stable and convective layers, respectively. When $s_m = s$, $q_m = i\hat{q}$ and $\Delta z_m' = \Delta z_c$, the transfer matrix $\boldsymbol{T}_{m,m+1}$ in (2.15) can be written as

$$\hat{T}_{11} = \frac{1}{4} e^{-is\Delta z_c} \left\{ \left[2 + i \left(\frac{\hat{q}}{s} - \frac{s}{\hat{q}} \right) \right] e^{-\hat{q}\Delta z_c} + \left[2 - i \left(\frac{\hat{q}}{s} - \frac{s}{\hat{q}} \right) \right] e^{\hat{q}\Delta z_c} \right\}, \quad (2.65)$$

915 A125-18

$$\hat{T}_{12} = \frac{1}{4} \, \mathrm{e}^{\mathrm{i}s(z_m + z'_m)} \left\{ \left[\left(\frac{\hat{q}}{s} + \frac{s}{\hat{q}} \right) \right] \mathrm{e}^{-\hat{q}\Delta z_c} - \left[\left(\frac{\hat{q}}{s} + \frac{s}{\hat{q}} \right) \right] \mathrm{e}^{\hat{q}\Delta z_c} \right\}, \tag{2.66}$$

with $\hat{T}_{22}^* = \hat{T}_{11}$ and $\hat{T}_{21} = \hat{T}_{12}^*$. The eigenvalues of $\boldsymbol{T}_{m,m+1}$ are the roots of the following equation:

$$\lambda^2 - 2\mathrm{Re}(\hat{T}_{11})\lambda + 1 = 0. \tag{2.67}$$

Similarly, we can obtain a sufficient condition for efficient wave tunnelling if

$$\Delta_\lambda = \left[\frac{1}{2} (\mathrm{e}^{-\hat{q}\Delta z_c} + \mathrm{e}^{\hat{q}\Delta z_c}) \cos(s\Delta z_c) + \frac{1}{4} \left(\frac{\hat{q}}{s} - \frac{s}{\hat{q}} \right) (\mathrm{e}^{-\hat{q}\Delta z_c} - \mathrm{e}^{\hat{q}\Delta z_c}) \sin(s\Delta z_c) \right]^2 - 1, \tag{2.68}$$

and $\Delta_\lambda \leq 0$. It should be noted that $\Delta_\lambda \leq 0$ is only a necessary but not sufficient condition for efficient transmission. If $|\hat{q}|\Delta z_c \gg 0$, then Δ_λ is likely to be greater than zero. Therefore, the probability is higher at small $|\hat{q}|\Delta z_c$ for efficient transmission to take place.

By using similar technique as mentioned in § 2.1.2, we can find an analytical solution for the transmission ratio for the special case $|s|\Delta z_s = (\ell' + 1/2)\pi$ (so that $|s|\Delta z_s - \pi/2 = \ell'\pi$ and $\hat{T}_{12}/\exp(\pi/2)$ is a pure imaginary number, and the problem is analogous to that in § 2.1.2). Here, we only give the result without showing the details. Under the condition $|s|\Delta z_s = (\ell' + 1/2)\pi$, the transmission ratio in the multi-layer structure for tunnelling of a gravity wave is

$$\eta = \left\{ \cos^2 M\beta + \frac{1}{4} \left[\left(\frac{\hat{q}}{s} - \frac{s}{\hat{q}} \right) (\mathrm{e}^{-\hat{q}\Delta z_c} + \mathrm{e}^{\hat{q}\Delta z_c}) \right]^2 \left[\left(\frac{\hat{q}}{s} + \frac{s}{\hat{q}} \right)^2 \right. \right.$$
$$\left. \left. - (\mathrm{e}^{-\hat{q}\Delta z_c} + \mathrm{e}^{\hat{q}\Delta z_c})^2 \right]^{-1} \sin^2 M\beta \right\}^{-1}, \tag{2.69}$$

where

$$\beta = \arg \left((\mathrm{e}^{-\hat{q}\Delta z_c} + \mathrm{e}^{\hat{q}\Delta z_c}) + \mathrm{i} \left[\left(\frac{\hat{q}}{s} + \frac{s}{\hat{q}} \right)^2 - (\mathrm{e}^{-\hat{q}\Delta z_c} + \mathrm{e}^{\hat{q}\Delta z_c})^2 \right]^{1/2} \right), \tag{2.70}$$

and arg is the argument function operating on complex numbers. Note that $\sin^2 M\beta \propto (\hat{q}/s + s/\hat{q})^2 - (\mathrm{e}^{-\hat{q}\Delta z_c} + \mathrm{e}^{\hat{q}\Delta z_c})^2$, and there is no singularity problem in (2.69). From (2.69), we see that efficient tunnelling of gravity waves generally requires $|\hat{q}|\Delta z_c$ to be small. In the limit $|\hat{q}|\Delta z_c \to 0$, we find $\eta \to 1$. Thus, enhanced transmission of wave tunnelling can occur at $|\hat{q}|\Delta z_c \to 0$ and $|s|\Delta z_s = (\ell' + 1/2)\pi$. We call this phenomenon 'resonant tunnelling'.

Figure 8 shows contour plots of the transmission ratios for different N_{min}^2 in a 101-layer structure ($M = 50$). In this calculation, all of the stable layers are assumed to have the same degree of stratification (N_{min}^2) and thickness (Δz_s), and the convective layers are assumed to have the same thickness (Δz_c). The analysis of the three-layer structure shows that efficient transmission only occurs when Δz_c is small. The mathematical analysis on the eigenvalues of the transfer matrices also indicates that efficient transmission is more likely to take place when Δz_c is small. For this reason, we set $\Delta z_c = 0.1/|\hat{q}|$ for all the computed cases. From the figure, we see that the transmission ratio is insensitive to the degree of stratification. Instead, the thickness of Δz_s is more important. In our calculations,
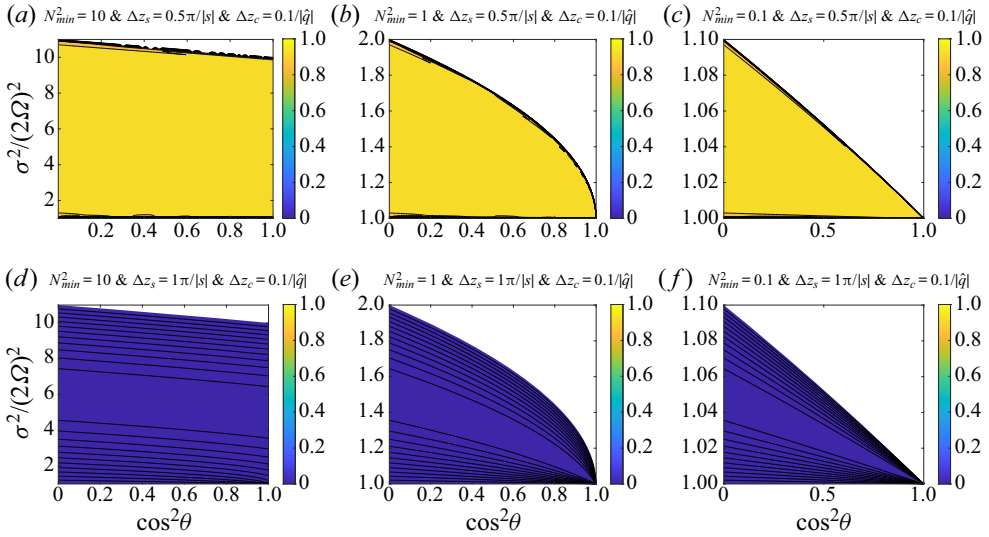
Figure 8. Contour plots of transmission ratios for the tunnelling of a gravity wave in a multi-layer structure. The buoyancy frequency and thicknesses of the convective layers are all the same with the values of N_{min}^2 and Δz_c, and the thicknesses of the stable layers are all the same with the value of Δz_s. (*a–c*) Transmission ratios when the buoyancy frequency $N_{min}^2 = 10, 1, 0.1, \Delta z_c = 0.1/|\hat{q}|$, and $\Delta z_s = 0.5\pi/|\hat{s}|$. (*d–f*) Transmission ratios when the buoyancy frequency $N_{min}^2 = 10, 1, 0.1, \Delta z_c = 0.1/|\hat{q}|$, and $\Delta z_s = \pi/|\hat{s}|$. Tunnelling of gravity waves can only occur in coloured regions. Regions are left white if tunnelling of gravity waves is prohibited.

we find that the transmission is efficient when $\Delta z_s = (\ell + 0.5)\pi/|s|$, and inefficient when $z_s = \ell\pi/|s|$, where ℓ is an integer. Therefore, the tunnelling of a gravity wave is efficient when each convective layer Δz_c is much shallower than the e-folding decay distance $1/|\hat{q}|$ and the thickness of each stable layer is close to a multiple-and-a-half of the half-wavelength.

2.2.2. *Tunnelling of inertial waves*

In this section, we discuss the tunnelling of inertial waves. Similarly, we consider a $(2M + 1)$-layer structure with alternating $M + 1$ convective layers and M stable layers. The plot is shown for configuration 4 in figure 6(*b*). For this configuration, an inertial wave can propagate in convective layers but no wave could propagate in stable layers, and thus the frequency range is $\sigma_1^2 < \sigma^2 < \sigma_2^2$. The width of the frequency domain is

$$\sigma_2^2 - \sigma_1^2 = \tfrac{1}{2}\left[(f^2 + \tilde{f}_s^2 + N_{min}^2) - \sqrt{(f^2 + \tilde{f}_s^2 + N_{min}^2)^2 - 4N_{min}^2 f^2} \right]. \tag{2.71}$$

Analysis shows that $\sigma_2^2 - \sigma_1^2$ decreases with θ and $\sin^2 \alpha$, and increases with $N_{min}^2/(2\Omega)^2$ (see Appendix C). Therefore, the frequency domain is wider at polar regions than equatorial regions. Also it is wider when the zonal wavenumber dominates the meridional wavenumber, and it is wider when the degree of stratification is stronger.

Now, we discuss the wave transmission of the tunnelling of an inertial wave. Again, we first consider a three-layer structure. It is not difficult to obtain the transmission
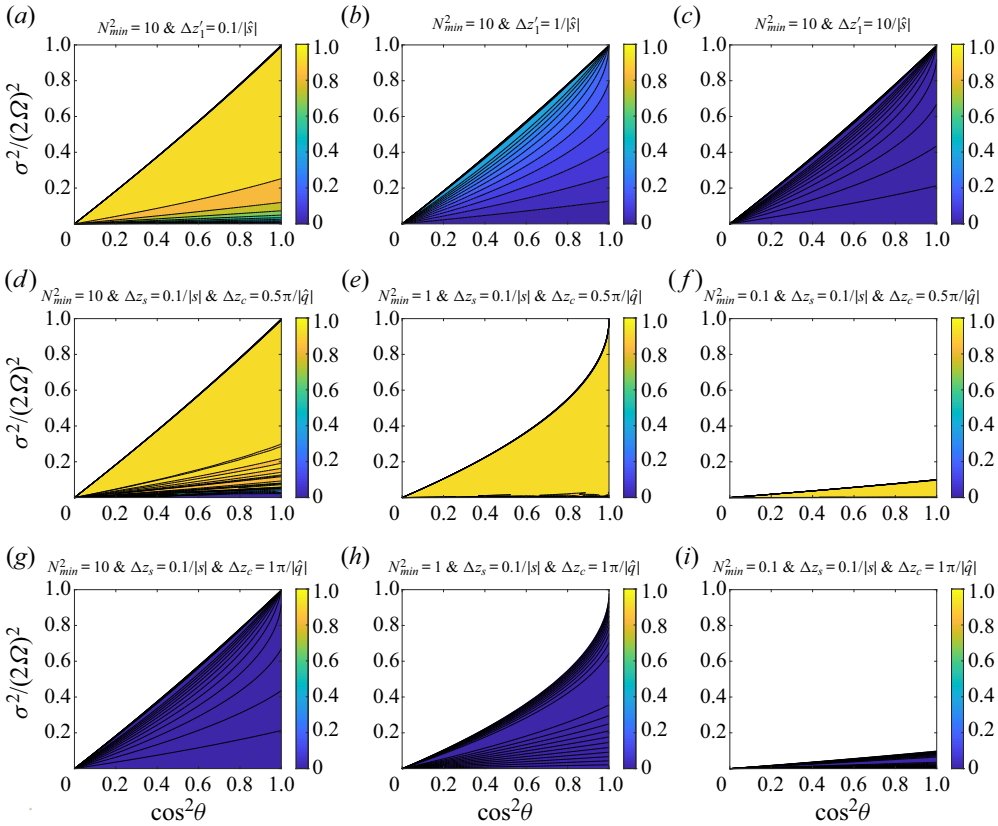
Figure 9. Contour plots of transmission ratios for the tunnelling of an inertial wave: (a,b,c) are for the three-layer structure; and $(d–i)$ are for the multi-layer structures. $(a–c)$ Transmission ratios for $N^2_{min} = 10$ and $\Delta z'_1 = (0.1, 1, 10)/|\hat{s}|$ in a three-layer structure. $(d–f)$ Transmission ratios for $N^2_{min} = (10, 1, 0.1)$, $\Delta z_c = 0.5\pi/|\hat{q}|$ and $\Delta z_s = 0.1/|s|$ in a 101-layer structure. $(g–i)$ Transmission ratios for $N^2_{min} = (10, 1, 0.1)$, $\Delta z_c = \pi/|\hat{q}|$ and $\Delta z_s = 0.1/|s|$ in a 101-layer structure. Tunnelling of inertial waves can only occur in coloured regions. Regions are left white if Tunnelling of gravity waves is prohibited.

ratio

$$
\eta = 16 \left\{ 4(e^{-\hat{s}_1 \Delta z'_1} + e^{\hat{s}_1 \Delta z'_1})^2 + \left[\left(\sqrt{\frac{\hat{s}^2_1}{q^2_1}} + \sqrt{\frac{q^2_1}{\hat{s}^2_1}} \right)^2 - 4 \right] \left[(e^{-\hat{s}_1 \Delta z'_1} + e^{\hat{s}_1 \Delta z'_1})^2 - 4 \right] \right\}^{-1} .
$$
(2.72)

Again, we can show that efficient transmission requires that the thickness of the stable layer is much smaller than the e-folding decay distance $1/|\hat{s}_1|$. Figure 9$(a–c)$ shows the transmission ratios in the three-layer structure when the stable layer is strongly stratified. It clearly shows that the transmission is only efficient when $\hat{s}_1 \Delta z'_1$ is small.

Now we discuss the tunnelling of an inertial wave in a structure with more layers. Similarly, we can use the recursive relations to calculate the transmission ratio. Here, we only give the result without showing details. Under the condition $|q|\Delta z_c = (\ell' + 1/2)\pi$, we find the transmission ratio of the tunnelling of inertial waves in a multi-layer

structure is

$$\eta = \left\{ \cos^2 M\beta + \frac{1}{4} \left[\left(\frac{\hat{s}}{q} - \frac{q}{\hat{s}} \right) (e^{-\hat{s}\Delta z_s} + e^{\hat{s}\Delta z_s}) \right]^2 \left[\left(\frac{\hat{s}}{q} + \frac{q}{\hat{s}} \right)^2 \right. \right.$$

$$\left. \left. - (e^{-\hat{s}\Delta z_s} + e^{\hat{s}\Delta z_s})^2 \right]^{-1} \sin^2 M\beta \right\}^{-1}, \tag{2.73}$$

where

$$\beta = \arg \left((e^{-\hat{s}\Delta z_s} + e^{\hat{s}\Delta z_s}) + i \left[\left(\frac{\hat{s}}{q} + \frac{q}{\hat{s}} \right)^2 - (e^{-\hat{s}\Delta z_s} + e^{\hat{s}\Delta z_s})^2 \right]^{1/2} \right). \tag{2.74}$$

Figure 9(*d–i*) shows the transmission ratios in a 101-layer structure. Again, we see that the efficiency of transmission mainly depends on the thicknesses of the convective and stable layers. For the transmission to be efficient, it requires that the thickness of stable layer (Δz_s) is much smaller than the e-folding decay distance $1/|\hat{s}|$, and the thickness of each convective layer is close to a multiple-and-a-half of the half-wavelength. This result is similar to that obtained in the tunnelling of gravity waves.

3. Non-traditional effects

Sutherland (2016) has discussed wave transmission in a multi-layer structure in traditional approximation. It is necessary to investigate the non-traditional effects on wave transmission in the multi-layer structure. Under the traditional approximation ($f_s^2 = 0$), the critical frequencies can be written as

$$\sigma_1^2 = 0, \quad \sigma_4^2 = f^2, \tag{3.1}$$

$$\sigma_2^2 = \min(f^2, N_{min}^2), \quad \sigma_5^2 = \max(f^2, N_{min}^2), \tag{3.2}$$

$$\sigma_3^2 = \min(f^2, N_{max}^2), \quad \sigma_6^2 = \max(f^2, N_{max}^2). \tag{3.3}$$

If stable layers are strongly stratified with $f^2 < N_{min}^2$, then $\sigma_2^2 = \sigma_3^2 = \sigma_4^2 = f^2, \sigma_5^2 = N_{min}^2$ and $\sigma_6^2 = N_{max}^2$. In such a case, a wave cannot propagate in both convective and stable layers, while tunnelling of gravity waves occurs at $f^2 < \sigma^2 < N_{min}^2$ and tunnelling of inertial waves occurs at $0 < \sigma^2 < f^2$ (see the upper panel of figure 10).

If stable layers are weakly stratified with $f^2 > N_{max}^2$, then $\sigma_4^2 = \sigma_5^2 = \sigma_6^2 = f^2, \sigma_2^2 = N_{min}^2$ and $\sigma_3^2 = N_{max}^2$. In such a case, tunnelling of gravity waves cannot occur, while a wave can propagate in both convective and stable layers at $N_{max}^2 < \sigma^2 < f^2$, and tunnelling of inertial waves occurs at $0 < \sigma^2 < N_{min}^2$ (see the lower panel of figure 10).

If the traditional approximation is made, wave propagation only occurs in weakly stratified flow, tunnelling of gravity waves only occurs in strongly stratified flow and tunnelling of inertial waves can occur in both strongly and weakly stratified flows. When non-traditional effects are included, however, no similar restriction is obtained in wave propagation or tunnelling. The non-traditional effects on wave propagation can already be seen by comparing figure 3(*a,d,g*) with figure 3(*b,c,e,f,h,i*). In the traditional approximation, $\tilde{f}_s$ is set to zero and this can be achieved by setting $\sin \alpha = 0$. Figure 3(*a,d,g*) shows transmission ratios with small $\tilde{f}_s$, which are similar to situations with
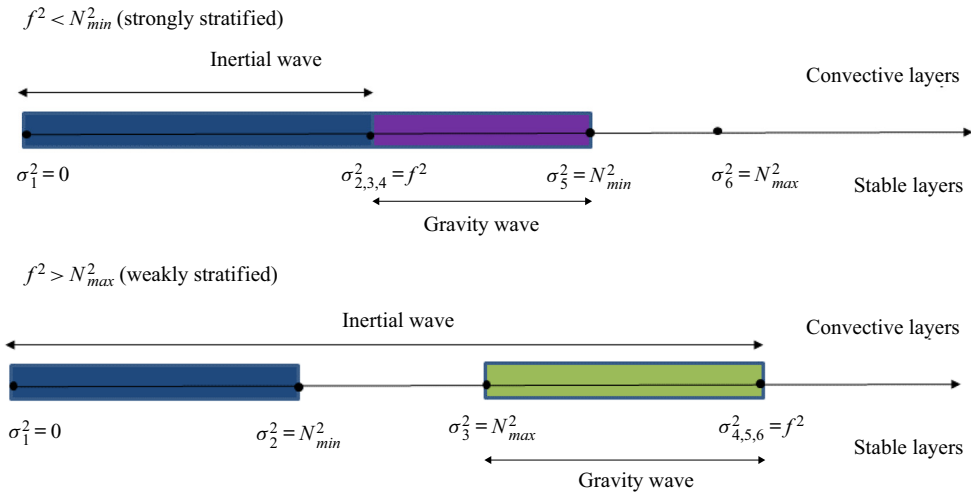
Figure 10. Plots of wave propagation in multiple convectively stable and unstable layers. Wave frequency ranges are shown above and below the middle arrow for convective and stable layers, respectively. Wave propagation occurs in the green region, tunnelling of inertial wave occurs in the blue region and tunnelling of gravity wave occurs in the purple region.

traditional approximation. If $\tilde{f}_s = 0$, the coloured regions in figure 3(a,d) vanish because wave propagation is prohibited when $N_{max}^2 \geq f^2$; and the coloured region in figure 3(c) will shrink into a triangle region below the diagonal line $\sigma^2/(2\Omega)^2 = \cos^2\theta$ (see figure 11a). For weakly stratified flow ($N_{max}^2 < f^2$), only sub-inertial waves ($\sigma^2 < f^2$) can propagate with the traditional approximation. However, super-inertial waves ($\sigma^2 > f^2$) can propagate if non-traditional effects are taken into account.

With the traditional approximation, tunnelling of gravity waves can only occur when stable layers are strongly stratified ($N_{min}^2 > f^2$), and the wave frequency is smaller than buoyancy frequency ($\sigma^2 < N_{min}^2$). When non-traditional effects are present, we see from figure 8 that tunnelling of gravity waves can occur when stable layers are weakly stratified. Also, tunnelling of gravity waves is possible for super-buoyancy-frequency waves.

For tunnelling of inertial waves, comparing figure 11(c–e) with figure 9(d–f), we see that frequency ranges are overestimated in the traditional approximation. This is especially true when stable layers are weakly stratified. From figures 11(c) and 9(d), we also see that the traditional approximation has a moderate effect on the transmission ratio in the small frequency range.

4. Summary

In this paper, we have investigated wave transmissions in rotating stars or planets with multiple radiative and convective zones. Two situations have been considered: wave propagation and wave tunnelling. For wave propagation, waves could propagate in both convective and stable layers. Previous studies on wave propagation in a two-layer structure with a step function of stratification (Wei 2020a; Cai *et al.* 2021) have shown that wave transmission is generally not efficient when the stable layer is strongly stratified (this is a typical behaviour despite the fact that transmission can be efficient under certain conditions, such as at the critical latitude). In this work, however, we find that the wave
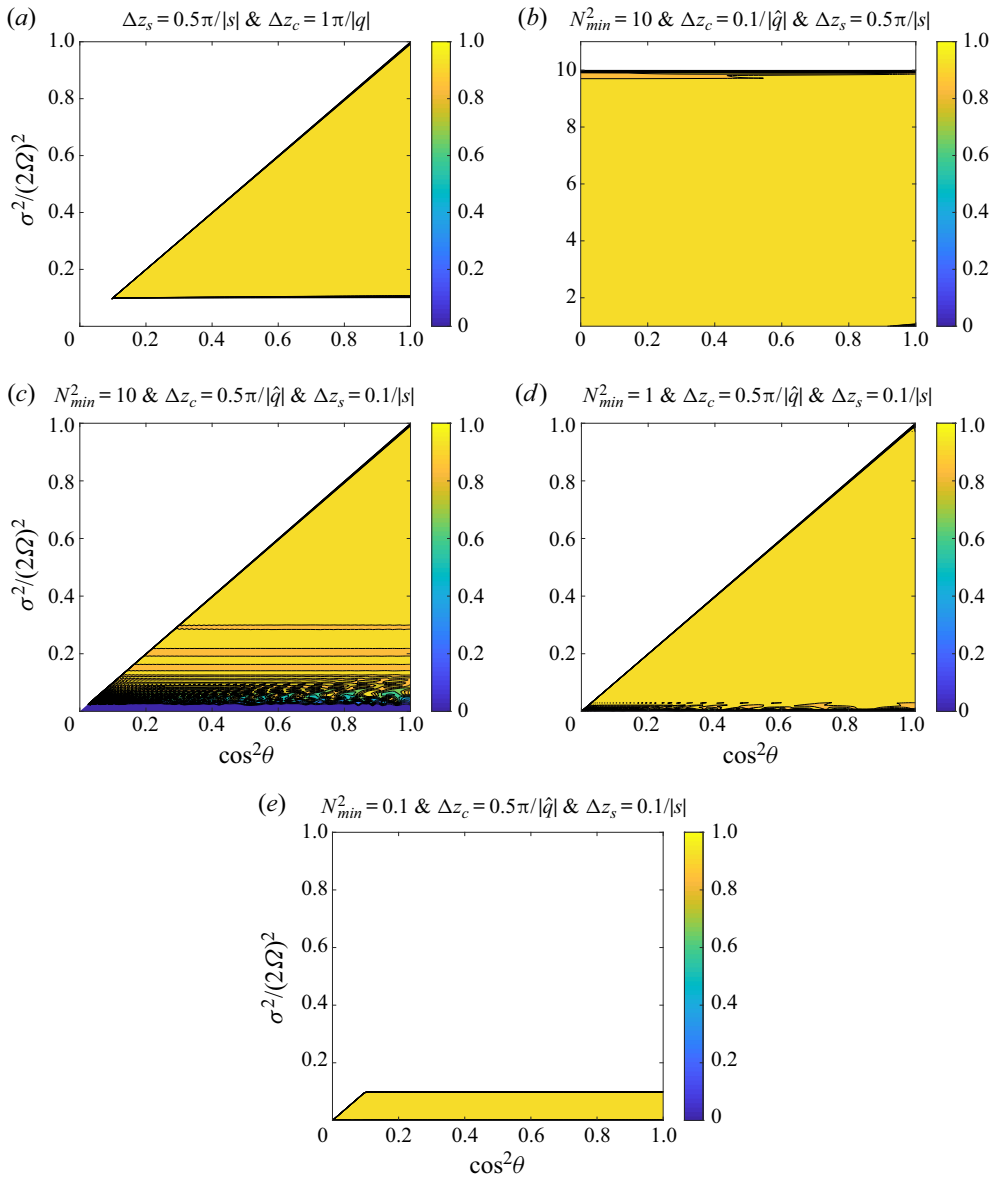
Figure 11. Wave transmissions with the traditional approximation. (*a*) Transmission for wave propagation. The setting is identical to that of figure 3(*g*) except that $\tilde{f}_s^2 = 0$ here. (*b*) Tunnelling of gravity waves. The setting is the same as that in figure 8(*a*) except that $\tilde{f}_s^2 = 0$ here. (*c–e*) Tunnelling of inertial waves. The settings are the same as those in figure 9(*d–f*) except that $\tilde{f}_s^2 = 0$ here. Coloured and white regions have similar meanings as those mentioned in previous contour plots.

transmission can be enhanced in a multiple-layer structure even though the stable layers are strongly stratified. We call this phenomenon 'enhanced wave transmission'. Enhanced wave transmission can only occur when the top and bottom layers are both convective layers or stable layers. We have the following major findings on wave propagation:

915 A125-24

  (i) In a three-layer structure, transmission can be enhanced when the top and bottom
      layers (clamping layers) have a similar buoyancy frequency, and the thickness of the
      middle layer is close to a multiple of the half-wavelength of the propagating wave
      inside this layer.
 (ii) Enhancement of transmission can also take place in a multi-layer structure under
      similar conditions when clamping layers have similar properties, the thickness of
      each clamping layer is close to a multiple of the half-wavelength of the propagating
      wave and the total thickness of each embedded layer is close to a multiple of
      the half-wavelength of the propagating wave. Efficient transmission can take place
      even when stable layers are strongly stratified. We call this phenomenon 'resonant
      propagation'.

For wave tunnelling, there are two cases: the tunnelling of a gravity wave, and the
tunnelling of an inertial wave. In the first case, waves can propagate in stable layers but
are evanescent in convective layers. In the second case, on the other hand, waves can
propagate in convective layers but are evanescent in stable layers. We have the following
major findings on wavetunnelling:

  (i) The tunnelling of a gravity wave can be efficient when stable layers have similar
      buoyancy frequencies, the thickness of each embedded convective layer is much
      smaller than the corresponding e-folding decay distance and the thickness of each
      stable layer is close to a multiple-and-a-half of the half-wavelength. The latter
      condition is unnecessary if the structure is three layered. We call this 'resonant
      tunnelling of gravity waves'.
 (ii) The tunnelling of an inertial wave can be efficient when stable layers have similar
      buoyancy frequencies, the thickness of each stable layer is much smaller than the
      corresponding e-folding decay distance and each convective layer thickness is close
      to a multiple-and-a-half of the half-wavelength. The latter condition is unnecessary
      if the structure is three layered. We call this 'resonant tunnelling of inertial waves'.
(iii) The efficiency of the tunnelling mainly depends on the layer thicknesses, the
      wavelengths and the e-folding decay distances.

It would be interesting to investigate the tunnelling of gravity waves in a non-rotating
fluid. This is a special case with $f = 0$ and $\widetilde{f_s} = 0$. In such a case, we can easily obtain
that $\hat{q}_m^2 = k^2$ and $s_m^2 = (N_m^2/\sigma^2 - 1)k^2$, where $\sigma^2 < N_m^2$. Then the conclusion (i) can be
directly applied to this special case.

Table 1 summarizes conditions for efficient transmissions of wave propagation and
tunnelling when all stable layers have similar buoyancy frequencies. For tunnelling waves,
clamping layers should have similar properties. Table 1 only lists the conditions in such
structures. The first column of table 1 lists four types of wave transmission: propagation
with convective layers embedded, propagation with stable layers embedded, tunnelling of
gravity waves and tunnelling of inertial waves. The second column gives the frequency
ranges. The third and fourth columns show the conditions for efficient transmission. From
the table, we see that the conditions for efficient wave transmission are significantly
different among tunnelling and propagative waves.

Our findings have interesting implications for gaseous planets. In a multi-layer structure,
Belyaev *et al.* (2015) found that the g-mode with vertical wavelengths smaller than
the layer thickness are evanescent in gaseous planets. This is true for tunnelling of

	σ^2	Δz_c	Δz_s
Propagation with CLs embedded in SLs	(σ_3^2, σ_4^2)	$M\Delta z_c \sim \ell\lambda_c/2$	$\Delta z_s \sim \ell'\lambda_s/2$
Propagation with SLs embedded in CLs	(σ_3^2, σ_4^2)	$\Delta z_c \sim \ell'\lambda_c/2$	$M\Delta z_s \sim \ell\lambda_s/2$
tunnelling of GWs	(σ_4^2, σ_5^2)	$\Delta z_c \ll \lambda_c$	$\Delta z_s \sim (\ell+1/2)\lambda_s/2$
tunnelling of IWs	(σ_1^2, σ_2^2)	$\Delta z_c \sim (\ell+1/2)\lambda_c/2$	$\Delta z_s \ll \lambda_s$

Table 1. Summary on efficient wave transmissions in a multi-layer structure.

Note: λ_c is the wavelength or decay distance in the convective layer; λ_s is the wavelength or decay distance in the stable layer; Δz_c and Δz_s are the thicknesses of the convective and stable layers, respectively; M is the number of embedded layers; ℓ and ℓ' are non-negative integers. IW and GW denote inertial and gravity waves, respectively. CLs and SLs denote convective and stable layers, respectively. Here, we only consider the situation that all stable layers have similar buoyancy frequencies, and clamping layers have similar properties.

g-mode waves. However, if considering wave propagation, g-mode waves can transmit efficiently even when the wavelength is smaller than the layer thickness. André *et al.* (2017) have made promising progress in the study of wave transmission in multi-layer structures, which reveals that wave transmission can be enhanced when the incident wave is resonant with waves in adjacent layers with half-wavelengths equal to the layer depth. Their result is consistent with our derivations. By deriving a group of exact solutions for wave transmission coefficients in multi-layer structures, we provide a mathematical explanation for why the transmission can be enhanced in a multi-layer structure. In addition, our analysis shows that wave transmission can also be enhanced in tunnelling of gravity waves or inertial waves. Conditions on 'resonant propagation' and 'resonant tunnelling' have been provided. Pontin *et al.* (2020) have conducted interesting research on wave propagation in a multi-layer structure in a non-rotating sphere, and found that wave transmissions are efficient for very large wavelength waves. This already shares some similarities with our analysis on the tunnelling of gravity waves in the f-plane. It has to be emphasized that our model is derived under the assumptions in the local f-plane. Application of the results to a global sphere should be performed with caution for the following reasons. First, only short wavelengths are considered in the local model. Wave transmissions of global scale waves have not been discussed. Second, the geometrical effect has not been taken into account. This is important for waves propagating in a global sphere. For example, super-inertial waves propagating from the equator to the poles may change to sub-inertial waves across critical colatitudes, where waves can also be transmitted or reflected in the meridional direction (Rieutord & Valdettaro 1997; Rieutord, Georgeot & Valdettaro 2001; Gerkema & Shrira 2005*a*; Shrira & Townsend 2010). Extending our work to a full spherical geometry will be a direction of improvement in the future.

Our findings may also have implications for the Earth's oceans, and in stars. It has been observed that there exists a multi-layer structure in theArctic Ocean, with thin stratified layers separated by mixed layers created by double diffusion (Rainville & Winsor 2008). By performing a joint theoretical and experimental study, Ghaemsaidi *et al.* (2016) revealed that the Arctic Ocean has a rich transmission behaviour. With their data, we can have a simple estimation on wave transmission in the Arctic Ocean by using our model. For the structure of the Arctic Ocean presented in Ghaemsaidi *et al.* (2016), N in stratified layers is approximately $1.6 \times 10^{-3} - 3.2 \times 10^{-3}$ s^{-1}; the inertial frequency f is approximately 1.4×10^{-4} s^{-1}; the thicknesses of embedded convective layers are of $O(1)$; the total depth of the multi-layer structure is approximately 30 m, which is

approximately separated into 14 stable layers. Since $N \gg f$, gravity waves are expected to transport across the multi-layer structure by tunnelling. From table 1, we see that waves with wavelength $\lambda_s \sim 8.6$ m can be transmitted efficiently by resonant tunnelling. Near-inertial waves with wavelengths 10–50 m can also transmit efficiently. This has been verified in Ghaemsaidi *et al.* (2016). Double diffusion also occurs in stars. Our model may also provide some insights into wave transmission in stars. The interior structures are different for different types of stars. For example, as studied in Cai (2014), late-type stars have a convectively stable–unstable–stable three-layer structure; A–F type stars generally have complicated internal structures with two separated convectively unstable layers (for example, some of them have a unstable–stable–unstable three-layer structure, and some of them have a stable–unstable–stable–unstable–stable five-layer structure), and massive stars have a unstable–stable two-layer structure. For waves excited at the innermost layer, resonant wave propagation from the innermost to the outermost layers can probably take place in late-type and A–F stars since the top and bottom layers are both convectively stable or unstable. However, if waves are excited in the second innermost layer, enhanced wave transmission is unlikely to occur from this layer to the outermost layer, because the bottom and top layers of the interested region are different. For massive stars, enhanced wave transmission is unlikely to take place because the properties of the top and bottom layers are different. We have to mention that the stratified structure specified in our model is ideal. In our Boussinesq model, density variation and viscous effects have been ignored. In real stars, however, density variation and viscous effects may be important. In addition, our model assumes that the buoyancy frequency changes abruptly across interfaces between convective and stable layers. For real stars, the change is likely to be smoother. Previous investigations of wave transmission in two-layer structures with smoothly varying buoyancy frequencies have shown significant differences. Models with more realistic settings are desirable in the future.

Author ORCIDs.

Tao Cai https://orcid.org/0000-0003-3431-8570;

Cong Yu https://orcid.org/0000-0003-0454-7890;

Xing Wei https://orcid.org/0000-0002-8033-2974.

Appendix A

Equations (2.11)–(2.14) can be written in a matrix form

$$\boldsymbol{S}_m \begin{bmatrix} a_m \\ b_m \end{bmatrix} = \boldsymbol{\Lambda}_m \boldsymbol{Q}_m \begin{bmatrix} c_m \\ d_m \end{bmatrix}, \tag{A1}$$

$$\tilde{\boldsymbol{\Lambda}}_m \tilde{\boldsymbol{Q}}_m \begin{bmatrix} c_m \\ d_m \end{bmatrix} = \tilde{\boldsymbol{S}}_m \begin{bmatrix} a_{m+1} \\ b_{m+1} \end{bmatrix}, \tag{A2}$$

where

$$\boldsymbol{S}_m = \begin{bmatrix} \mathrm{e}^{-\mathrm{i}s_m z_m} & \mathrm{e}^{\mathrm{i}s_m z_m} \\ -\mathrm{e}^{-\mathrm{i}s_m z_m} & \mathrm{e}^{\mathrm{i}s_m z_m} \end{bmatrix}, \quad \boldsymbol{Q}_m = \begin{bmatrix} \mathrm{e}^{-\mathrm{i}q_m z_m} & \mathrm{e}^{\mathrm{i}q_m z_m} \\ -\mathrm{e}^{-\mathrm{i}q_m z_m} & \mathrm{e}^{\mathrm{i}q_m z_m} \end{bmatrix},$$

$$\boldsymbol{\Lambda}_m = \begin{bmatrix} 1 & 0 \\ 0 & q_m/s_m \end{bmatrix}, \tag{A3}$$

$$\tilde{\boldsymbol{S}}_m = \begin{bmatrix} \mathrm{e}^{-\mathrm{i}s_{m+1} z'_m} & \mathrm{e}^{\mathrm{i}s_{m+1} z'_m} \\ -\mathrm{e}^{-\mathrm{i}s_{m+1} z'_m} & \mathrm{e}^{\mathrm{i}s_{m+1} z'_m} \end{bmatrix}, \quad \tilde{\boldsymbol{Q}}_m = \begin{bmatrix} \mathrm{e}^{-\mathrm{i}q_m z'_m} & \mathrm{e}^{\mathrm{i}q_m z'_m} \\ -\mathrm{e}^{-\mathrm{i}q_m z'_m} & \mathrm{e}^{\mathrm{i}q_m z'_m} \end{bmatrix},$$

$$\tilde{\boldsymbol{\Lambda}}_m = \begin{bmatrix} 1 & 0 \\ 0 & q_m/s_{m+1} \end{bmatrix}. \tag{A4}$$

Synthesizing these equations, we obtain the recursive relation

$$\begin{bmatrix} a_m \\ b_m \end{bmatrix} = \boldsymbol{T}_{m,m+1} \begin{bmatrix} a_{m+1} \\ b_{m+1} \end{bmatrix}, \tag{A5}$$

where the transfer matrix

$$\boldsymbol{T}_{m,m+1} = \boldsymbol{S}_m^{-1} \boldsymbol{\Lambda}_m \boldsymbol{Q}_m \tilde{\boldsymbol{Q}}_m^{-1} \tilde{\boldsymbol{\Lambda}}_m^{-1} \tilde{\boldsymbol{S}}_m = \begin{bmatrix} \hat{T}_{11} & \hat{T}_{12} \\ \hat{T}_{21} & \hat{T}_{22} \end{bmatrix}, \tag{A6}$$

and

$$\hat{T}_{11} = \frac{1}{4} \mathrm{e}^{\mathrm{i}(s_m z_m - s_{m+1} z'_m)} \left[\left(1 + \frac{q_m}{s_m} + \frac{s_{m+1}}{s_m} + \frac{s_{m+1}}{q_m} \right) \mathrm{e}^{\mathrm{i}q_m \Delta z'_m} \right.$$
$$\left. + \left(1 - \frac{q_m}{s_m} + \frac{s_{m+1}}{s_m} - \frac{s_{m+1}}{q_m} \right) \mathrm{e}^{-\mathrm{i}q_m \Delta z'_m} \right], \tag{A7}$$

$$\hat{T}_{12} = \frac{1}{4} \mathrm{e}^{\mathrm{i}(s_m z_m + s_{m+1} z'_m)} \left[\left(1 + \frac{q_m}{s_m} - \frac{s_{m+1}}{s_m} - \frac{s_{m+1}}{q_m} \right) \mathrm{e}^{\mathrm{i}q_m \Delta z'_m} \right.$$
$$\left. + \left(1 - \frac{q_m}{s_m} - \frac{s_{m+1}}{s_m} + \frac{s_{m+1}}{q_m} \right) \mathrm{e}^{-\mathrm{i}q_m \Delta z'_m} \right], \tag{A8}$$

with $\hat{T}_{21} = \hat{T}_{12}^*$ and $\hat{T}_{22} = \hat{T}_{11}^*$.

Appendix B

For the tunnelling of a gravity wave, the width of the frequency domain is

$$\sigma_5^2 - \sigma_4^2 = \frac{1}{2} \left[(N_{min}^2 - f^2 - \tilde{f}_s^2) + \sqrt{(N_{min}^2 - f^2 - \tilde{f}_s^2)^2 + 4N_{min}^2 \tilde{f}_s^2} \right]. \tag{B1}$$

The monotonicity of the frequency width is equivalent to that of the function

$$G(\theta, \mu_1, \mu_2) = G_1(\theta, \mu_1, \mu_2) + \sqrt{G_1^2(\theta, \mu_1, \mu_2) + 4G_2(\theta, \mu_1, \mu_2)}, \tag{B2}$$

where $G_1(\theta, \mu_1, \mu_2) = \mu_2 - \cos^2\theta - \mu_1 \sin^2\theta$, $G_2(\theta, \mu_1, \mu_2) = \mu_1\mu_2 \sin^2\theta$, $\mu_1 = \sin^2\alpha$ and $\mu_2 = N^2_{min}/(2\Omega)^2$. To analyse the monotonicity of $G(\theta, \mu_1, \mu_2)$ on θ, we compute

$$G_\theta = G_{1\theta} + \frac{G_1 G_{1\theta} + 2G_{2\theta}}{\sqrt{G_1^2 + 4G_2}}. \tag{B3}$$

Because $G_{1\theta} = \sin 2\theta(1 - \mu_1) > 0$ and $G_{2\theta} = \mu_1\mu_2 \sin 2\theta > 0$, we have

$$G_\theta = \frac{\left(\sqrt{G_1^2 + 4G_2} + G_1\right) G_{1\theta} + 2G_{2\theta}}{\sqrt{G_1^2 + 4G_2}} \geq 0. \tag{B4}$$

Therefore, the frequency width always increases with θ.

To analyse the monotonicity of G on μ_1, we compute

$$G_{\mu_1} = G_{1\mu_1} + \frac{G_1 G_{1\mu_1} + 2G_{2\mu_1}}{\sqrt{G_1^2 + 4G_2}} \tag{B5}$$

$$= -\sin^2\theta + \frac{\sqrt{G_1^2 + 4G_2 + 4\mu_2 \cos^2\theta}}{\sqrt{G_1^2 + 4G_2}} \sin^2\theta \geq 0. \tag{B6}$$

Therefore, the frequency width always increases with μ_1.

To analyse the monotonicity of G on μ_2, we compute

$$G_{\mu_2} = G_{1\mu_2} + \frac{G_1 G_{1\mu_2} + 2G_{2\mu_2}}{\sqrt{G_1^2 + 4G_2}} \tag{B7}$$

$$= \frac{\sqrt{G_1^2 + 4G_2} + G_1 + 2\mu_1 \sin^2\theta}{\sqrt{G_1^2 + 4G_2}} > 0. \tag{B8}$$

Therefore, the frequency width always increases with μ_2.

Appendix C

For the tunnelling of an inertial wave, the width of the frequency domain is

$$\sigma_2^2 - \sigma_1^2 = \frac{1}{2}\left[(f^2 + \tilde{f}_s^2 + N^2_{min}) - \sqrt{(f^2 + \tilde{f}_s^2 + N^2_{min})^2 - 4N^2_{min}f^2}\right]. \tag{C1}$$

The monotonicity of the frequency width is equivalent to that of the function

$$H(\theta, \mu_1, \mu_2) = H_1(\theta, \mu_1, \mu_2) - \sqrt{H_1^2(\theta, \mu_1, \mu_2) - 4H_2(\theta, \mu_1, \mu_2)}, \tag{C2}$$

where $H_1(\theta, \mu_1, \mu_2) = \mu_2 + \cos^2\theta + \mu_1 \sin^2\theta$, $H_2(\theta, \mu_1, \mu_2) = \mu_2 \cos^2\theta$, $\mu_1 = \sin^2\alpha$ and $\mu_2 = N^2_{min}/(2\Omega)^2$. The derivative of $H(\theta, \mu_1, \mu_2)$ to θ is

$$H_\theta = H_{1\theta} - \frac{H_1 H_{1\theta} - 2H_{2\theta}}{\sqrt{H_1^2 - 4H_2}}. \tag{C3}$$

Since $H_{1\theta} = (\mu_1 - 1) \sin 2\theta$ and $H_{2\theta} = -\mu_2 \sin 2\theta$, we have

$$H_\theta = \frac{\left(\sqrt{H_1^2 - 4H_2} - H_1\right) H_{1\theta} + 2H_{2\theta}}{\sqrt{H_1^2 - 4H_2}} \le 0. \tag{C4}$$

Therefore, the width of the frequency domain decreases with θ. The derivative of $H(\theta, \mu_1, \mu_2)$ to μ_1 is

$$H_{\mu_1} = H_{1\mu_1} - \frac{H_1 H_{1\mu_1} - 2H_{2\mu_1}}{\sqrt{H_1^2 - 4H_2}}. \tag{C5}$$

Since $H_{1\mu_1} = \sin^2 \theta$ and $H_{2\mu_1} = 0$, we have

$$H_{\mu_1} = \frac{\left(\sqrt{H_1^2 - 4H_2} - H_1\right) \sin^2 \theta}{\sqrt{H_1^2 - 4H_2}} \le 0. \tag{C6}$$

Therefore, the width of the frequency domain decreases with μ_1. The derivative of $H(\theta, \mu_1, \mu_2)$ to μ_2 is

$$H_{\mu_2} = H_{1\mu_2} - \frac{H_1 H_{1\mu_2} - 2H_{2\mu_2}}{\sqrt{H_1^2 - 4H_2}}. \tag{C7}$$

Since $H_{1\mu_2} = 1$ and $H_{2\mu_2} = \cos^2 \theta$, we have

$$H_{\mu_2} = \frac{\sqrt{H_1^2 - 4H_2} - H_1 + 2\cos^2 \theta}{\sqrt{H_1^2 - 4H_2}}. \tag{C8}$$

It is found that

$$H_1^2 - 4H_2 - (H_1 - 2\cos^2 \theta)^2 = \mu_1 \sin^2 2\theta \ge 0, \tag{C9}$$

then we have

$$H_{\mu_2} \ge 0. \tag{C10}$$

Thus, the width of the frequency domain increases with μ_2.

REFERENCES

AERTS, C., MATHIS, S. & ROGERS, T.M. 2019 Angular momentum transport in stellar interiors. *Annu. Rev. Astron. Astrophys.* **57**, 35–78.

ANDRÉ, Q., BARKER, A.J. & MATHIS, S. 2017 Layered semi-convection and tides in giant planet interiors-I. Propagation of internal waves. *Astron. Astrophys.* **605**, A117.

BELKACEM, K., MARQUES, J.P., GOUPIL, M.J., SONOI, T., OUAZZANI, R.M., DUPRET, M.-A., MATHIS, S., MOSSER, B. & GROSJEAN, M. 2015a Angular momentum redistribution by mixed modes in evolved low-mass stars-I. Theoretical formalism. *Astron. Astrophys.* **579**, A30.

BELKACEM, K., MARQUES, J.P., GOUPIL, M.J., SONOI, T., OUAZZANI, R.M., DUPRET, M.-A., MATHIS, S., MOSSER, B. & GROSJEAN, M. 2015b Angular momentum redistribution by mixed modes in evolved low-mass stars-II. Spin-down of the core of red giants induced by mixed modes. *Astron. Astrophys.* **579**, A31.

BELYAEV, M.A., QUATAERT, E. & FULLER, J. 2015 The properties of g-modes in layered semiconvection. *Mon. Not. R. Astron. Soc.* **452** (3), 2700–2711.

CAI, T. 2014 Numerical analysis of non-local convection. *Mon. Not. R. Astron. Soc.* **443** (4), 3703–3711.

CAI, T., YU, C. & WEI, X. 2021 Inertial and gravity wave transmissions near radiative-convective boundaries. *J. Fluid Mech.* (accepted) arXiv:2008.00205.

FULLER, J. 2014 Saturn ring seismology: evidence for stable stratification in the deep interior of saturn. *Icarus* **242**, 283–296.

GARAUD, P. 2018 Double-diffusive convection at low Prandtl number. *Annu. Rev. Fluid Mech.* **50**, 275–298.

GERKEMA, T. & EXARCHOU, E. 2008 Internal-wave properties in weakly stratified layers. *J. Mar. Res.* **66** (5), 617–644.

GERKEMA, T. & SHRIRA, V.I. 2005a Near-inertial waves on the nontraditional β plane. *J. Geophys. Res.: Oceans* **110**, C10003.

GERKEMA, T. & SHRIRA, V.I. 2005b Near-inertial waves in the ocean: beyond the "traditional approximation". *J. Fluid Mech.* **529**, 195–219.

GHAEMSAIDI, S.J., DOSSER, H.V., RAINVILLE, L. & PEACOCK, T. 2016 The impact of multiple layering on internal wave transmission. *J. Fluid Mech.* **789**, 617–629.

GOODMAN, J. & LACKNER, C. 2009 Dynamical tides in rotating planets and stars. *Astrophys. J.* **696** (2), 2054–2067.

LECONTE, J. & CHABRIER, G. 2012 A new vision of giant planet interiors: impact of double diffusive convection. *Astron. Astrophys.* **540**, A20.

MIHALAS, D. & MIHALAS, B.W. 2013 *Foundations of Radiation Hydrodynamics*. Courier Corporation.

MIRALLES, J.A., URPIN, V. & VAN RIPER, K. 1997 Convection in the surface layers of neutron stars. *Astrophys. J.* **480** (1), 358–363.

MIROUH, G.M., GARAUD, P., STELLMACH, S., TRAXLER, A.L. & WOOD, T.S. 2012 A new model for mixing by double-diffusive convection (semi-convection). I. The conditions for layer formation. *Astrophys. J.* **750** (1), 61.

MOORE, K. & GARAUD, P. 2016 Main sequence evolution with layered semiconvection. *Astrophys. J.* **817** (1), 54.

OGILVIE, G.I. & LIN, D.N.C. 2004 Tidal dissipation in rotating giant planets. *Astrophys. J.* **610** (1), 477–509.

PINÇON, C., BELKACEM, K., GOUPIL, M.J. & MARQUES, J.P. 2017 Can plume-induced internal gravity waves regulate the core rotation of subgiant stars? *Astron. Astrophys.* **605**, A31.

PONTIN, C.M., BARKER, A.J., HOLLERBACH, R., ANDRÉ, Q. & MATHIS, S. 2020 Wave propagation in semiconvective regions of giant planets. *Mon. Not. R. Astron. Soc.* **493** (4), 5788–5806.

RAINVILLE, L. & WINSOR, P. 2008 Mixing across the arctic ocean: microstructure observations during the beringia 2005 expedition. *Geophys. Res. Lett.* **35**, L08606.

RIEUTORD, M., GEORGEOT, B. & VALDETTARO, L. 2001 Inertial waves in a rotating spherical shell: attractors and asymptotic spectrum. *J. Fluid Mech.* **435**, 103–144.

RIEUTORD, M. & VALDETTARO, L. 1997 Inertial waves in a rotating spherical shell. *J. Fluid Mech.* **341**, 77–99.

ROGERS, T.M., LIN, D.N.C. & LAU, H.H.B. 2012 Internal gravity waves modulate the apparent misalignment of exoplanets around hot stars. *Astrophys. J. Lett.* **758** (1), L6.

ROGERS, T.M., LIN, D.N.C., MCELWAINE, J.N. & LAU, H.H.B. 2013 Internal gravity waves in massive stars: angular momentum transport. *Astrophys. J.* **772** (1), 21.

SHRIRA, V.I. & TOWNSEND, W.A. 2010 Inertia-gravity waves beyond the inertial latitude. Part 1. Inviscid singular focusing. *J. Fluid Mech.* **664**, 478–509.

SILVERS, L.J. & PROCTOR, M.R.E. 2007 The interaction of multiple convection zones in A-type stars. *Mon. Not. R. Astron. Soc.* **380** (1), 44–50.

SINGH, Y. 2010 *Semiconductor Devices*. IK International Pvt Ltd.

SUTHERLAND, B.R. 1996 Internal gravity wave radiation into weakly stratified fluid. *Phys. Fluids* **8** (2), 430–441.

SUTHERLAND, B.R. 2016 Internal wave transmission through a thermohaline staircase. *Phys. Rev. Fluids* **1** (1), 013701.

SUTHERLAND, B.R. & YEWCHUK, K. 2004 Internal wave tunnelling. *J. Fluid Mech.* **511**, 125–134.

TELLMANN, S., PÄTZOLD, M., HÄUSLER, B., BIRD, M.K. & TYLER, G.L. 2009 Structure of the venus neutral atmosphere as observed by the radio science experiment vera on venus express. *J. Geophys. Res.: Planets* **114**, E00B36.

WEI, X. 2020a Wave reflection and transmission at the interface of convective and stably stratified regions in a rotating star or planet. *Astrophys. J.* **890** (1), 20.

WEI, X. 2020b Erratum: wave reflection and transmission at the interface of convective and stably stratified regions in a rotating star or planet (APJ, 2020, 890, 20). *Astrophys. J.* **899** (1), 88.

WOOD, T.S., GARAUD, P. & STELLMACH, S. 2013 A new model for mixing by double-diffusive convection (semi-convection). II. The transport of heat and composition through layers. *Astrophys. J.* **768** (2), 157.

WU, Y. 2005*a* Origin of tidal dissipation in Jupiter. I. Properties of inertial modes. *Astrophys. J.* **635** (1), 674–687.

WU, Y. 2005*b* Origin of tidal dissipation in Jupiter. II. The value of Q. *Astrophys. J.* **635** (1), 688–710.

ZHANG, K. & LIAO, X. 2017 *Theory and Modeling of Rotating Fluids: Convection, Inertial Waves and Precession*. Cambridge University Press.